

纳米研究 (英文版)



Q K 2 2 2 9 3 7 1

ISSN 1998-0124

CN 11-5974/O4

Nano Research

May · 2022
Volume 15 · Number 5

Organic photocatalysts: From molecular to aggregate level

Birefringent response of graphene oxide film structured via femtosecond laser

Emerging Internet of Things driven carbon nanotubes-based devices

ISSN 1998-0124



05 >

9 771998 012221

万方数据



TSINGHUA
UNIVERSITY PRESS



Springer



Contents

Catalytic

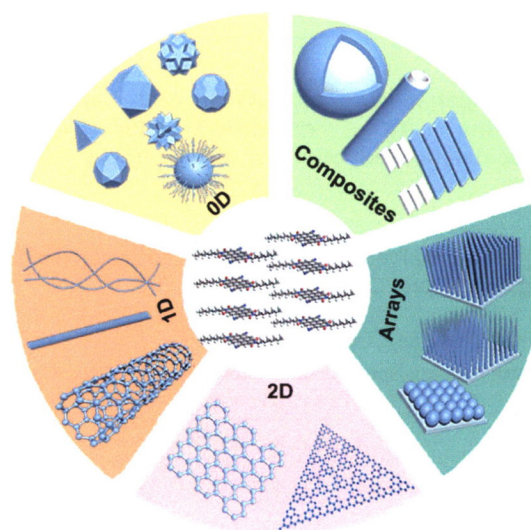
Review Article

Organic photocatalysts: From molecular to aggregate level

Chuxuan Yan¹, Jiaqi Dong¹, Yingzhi Chen^{1,2,*}, Wenjie Zhou², Yu Peng¹, Yue Zhang², and Lu-ning Wang^{1,2,*}

¹ University of Science and Technology Beijing, China

² Shunde Graduate School of University of Science and Technology Beijing, China



The ease of molecular modification and crystal/interface engineering allow organic photocatalysts to perform versatily in both homogeneous and heterogeneous photocatalysis. We review free organic molecules, supported organic molecules, and organic aggregates by discussing the lightabsorption properties, charge carrier behaviors, and configurational stability to achieve careful structure/property control for high-performance photocatalysis.

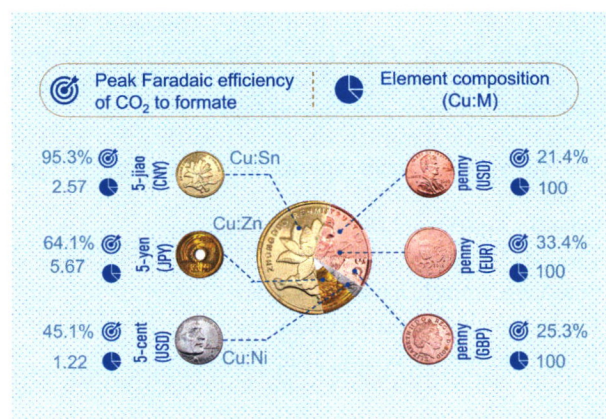
3835–3858

Research Articles

CO₂ reduction with coin catalyst

Taishi Xiao, Can Tang, Hongbin Li, Tong Ye, Kun Ba, Peng Gong, and Zhengzong Sun*

Fudan University, China



We successfully demonstrate the “third side of a coin” as an efficient CO₂ reduction catalyst. A closed-loop lifecycle of formate/formic acid was developed, promising as an industry-compatible commodity chemical.

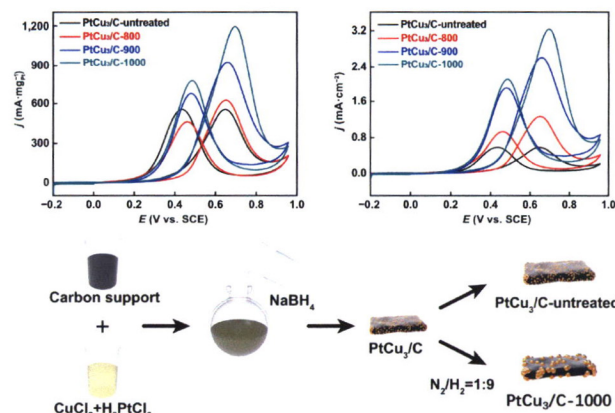
3859–3865

Structure engineering of PtCu₃/C catalyst from disordered to ordered intermetallic compound with heat-treatment for the methanol electrooxidation reaction

Zihao Xing¹, Jun Li¹, Shun Wang¹, Chenliang Su^{2,*}, and Huile Jin¹

¹ Wenzhou University, China

² Shenzhen University, China



The intermetallic compound of PtCu₃/C-1000 exhibited high specific activity of 3.23 mA·cm⁻¹ and mass activity of 1,200 mA·mg_{Pt}⁻¹ towards the methanol electrooxidation reaction.

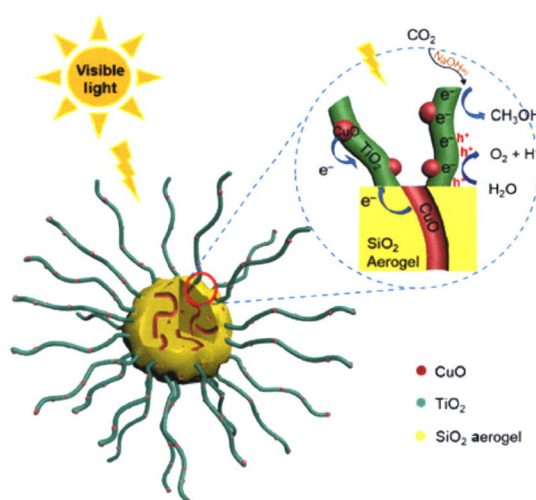
3866–3871

Hierarchical loading of CuO on SiO₂ aerogel@high crystalline TiO₂ nanofibers for efficiently photocatalytic reduction of CO₂ without sacrificial agent

Man Wen¹, Beibei Ren¹, Xiangzhi Ye¹, Jianxiong He², Hong Jiang¹, and Chunrong Xiong^{1,*}

¹ Hainan University, China

² Hainan haikong Special Glass Techology Co., Ltd., China



The high crystalline nanofibers and a hierarchical nanocomposite significantly enhanced the density and stability of photoexcited electron-hole pairs. The catalysts combined many advantageous features and exhibited an efficiently photocatalytic reduction of CO₂ without sacrificial agent.

3872–3879

Highly efficient two-electron electroreduction of oxygen into hydrogen peroxide over Cu-doped TiO₂

Zhiqin Deng¹, Li Li¹, Yuchun Ren¹, Chaoqun Ma², Jie Liang¹, Kai Dong¹, Qian Liu^{3,*}, Yonglan Luo³, Tingshuai Li¹, Bo Tang⁴, Yang Liu⁵, Shuyan Gao⁵, Abdullah M. Asiri⁶, Shihai Yan^{2,*}, and Xuping Sun^{1,*}

¹ University of Electronic Science and Technology of China, China

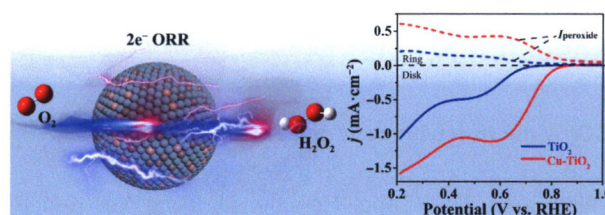
² Qingdao Agricultural University, China

³ Chengdu University, China

⁴ Shandong Normal University, China

⁵ Henan Normal University, China

⁶ King Abdulaziz University, Saudi Arabia



Cu acts as an effective dopant to boost the catalytic activity of TiO₂ for 2e⁻ O₂ reduction reaction. Such Cu-TiO₂ electrocatalyst achieves a high H₂O₂ selectivity of 91.2% and a large Faradaic efficiency (FE) of 98% in an alkaline medium.

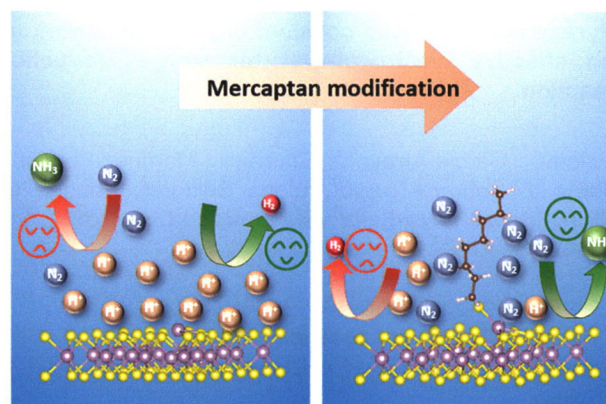
3880–3885

Surface hydrophobic modification enhanced catalytic performance of electrochemical nitrogen reduction reaction

Lijuan Niu¹, Ziwen Liu¹, Guohua Liu¹, Mengxuan Li², Xupeng Zong¹, Dandan Wang¹, Li An^{1,*}, Dan Qu¹, Xiaoming Sun¹, Xiayan Wang¹, and Zaicheng Sun^{1,*}

¹ Beijing University of Technology, China

² Jilin Normal University, China



MoS₂ after thiol modification increased the local N₂ concentration, inhibited the hydrogen reduction reaction (HER), and facilitated the adsorption of N₂, which further improved the nitrogen reduction reaction (NRR) activity.

3886–3893

Plasmon-mediated photodecomposition of NH₃ via intramolecular charge transfer

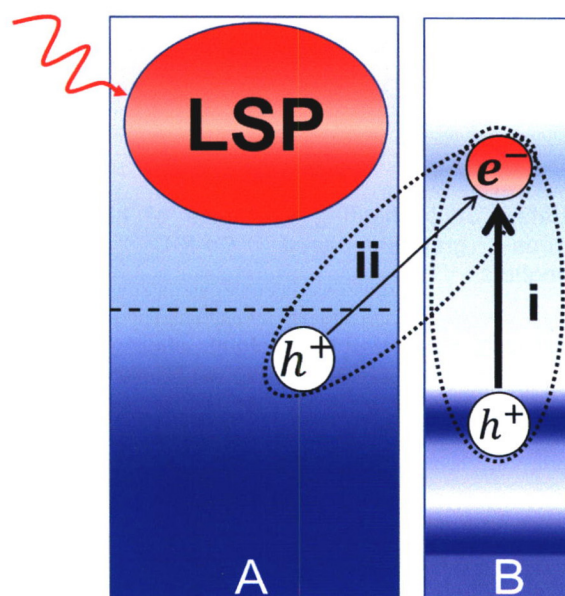
Yimin Zhang^{1,2,4}, Weite Meng^{2,3}, Daqiang Chen^{1,4}, Lili Zhang², Shunfang Li^{2,*}, and Sheng Meng^{1,4,*}

¹ Beijing National Laboratory for Condensed Matter Physics and Institute of Physics, Chinese Academy of Sciences, China

² Zhengzhou University, China

³ Anhui University of Science and Technology, China

⁴ University of Chinese Academy of Sciences, China



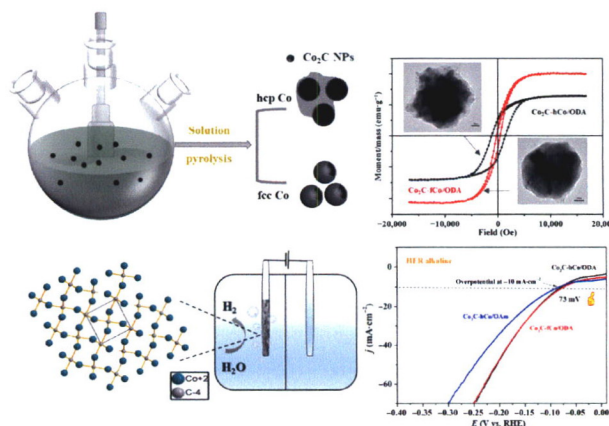
Intramolecular charge transfer induced by localized surface plasmon dominates the plasmon-mediated photolysis of NH₃, accompanying with a secondary direct charge transfer.

3894–3900

High coercivity cobalt carbide nanoparticles as electrocatalysts for hydrogen evolution reaction

Yaqin Qie, Yixuan Liu, Fanqi Kong, Zhilin Yang, and Hua Yang*

Jilin University, China



An improved solution pyrolysis route was used to synthesize single-phase cobalt carbides with high coercivity and excellent hydrogen evolution reaction (HER) catalytic activities, in which cobalt nanoparticles (NPs) with different structures were used as raw materials.

3901–3906

Pyrenetetraone-based covalent organic framework as an effective electrocatalyst for oxygen reduction reaction

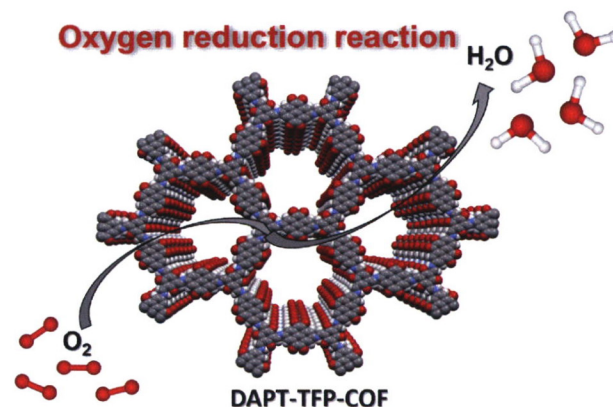
Paloma García-Arroyo¹, Emiliano Martínez-Periñán², Jorge J. Cabrera-Trujillo¹, Elena Salagre², Enrique G. Michel², José I. Martínez³, Encarnación Lorenzo^{2,4,*}, and José L. Segura^{1,*}

¹ Universidad Complutense de Madrid, Spain

² Universidad Autónoma de Madrid, Spain

³ Instituto de Ciencia de Materiales de Madrid (ICMM-CSIC), Spain

⁴ Instituto Madrileño de Estudios Avanzados en Nanociencia (IMDEA-Nanociencia), Spain



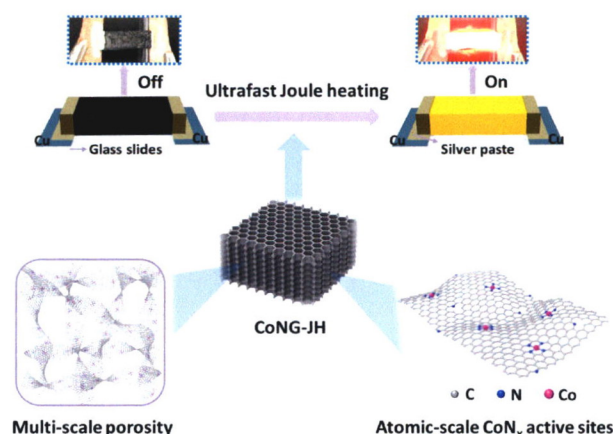
A novel two-dimensional (2D) covalent organic framework (DAPT-TFP-COF) was synthesized by incorporating highly electroactive pyrene-4,5,9,10-tetraone (PTO) units, which was tested as an electrocatalyst towards oxygen reduction reaction.

3907–3912

Ultrafast Joule heating synthesis of hierarchically porous graphene-based Co-N-C single-atom monoliths

Lingli Xing, Rui Liu, Zhichao Gong, Jingjing Liu, Jianbin Liu, Haisheng Gong, Kang Huang, and Huilong Fei*

Hunan University, China



The ultrafast Joule heating process ensures the rapid and stable dispersion of atomic-scale CoN_x active sites in graphene, while the three-dimensional hierarchically porous architecture promotes the mass transfer efficiency during the catalytic process.

3913–3919

Synergistic combination of Pd nanosheets and porous Bi(OH)₃ boosts activity and durability for ethanol oxidation reaction

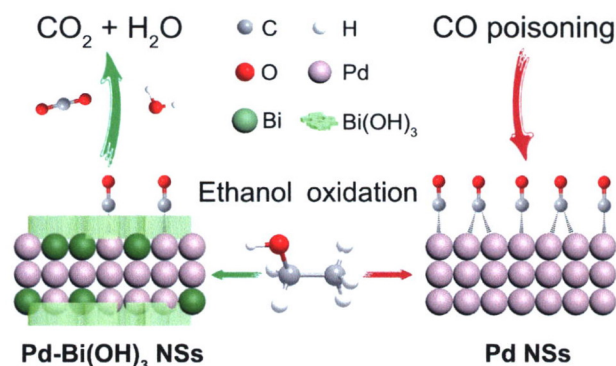
Mingyu Chu², Jialu Huang¹, Jin Gong², Yi Qu⁴, Guoling Chen⁴, Hu Yang¹, Xuchun Wang^{2,3}, Qixuan Zhong², Chengwei Deng^{4,*}, Muhan Cao², Jinxing Chen², Xiaolei Yuan^{1,2,*}, and Qiao Zhang²

¹ Nantong University, China

² Soochow University, China

³ University of Western Ontario, Canada

⁴ Shanghai Institute of Space Power-Sources, China



The incorporation of Bi(OH)₃ species effectively tunes the electronic (induce Pd into an electron-rich state) and geometric (separate the Pd ensemble) structures of Pd nanosheets, leading to the improved ethanol oxidation reaction (EOR) activity and superior CO tolerance.

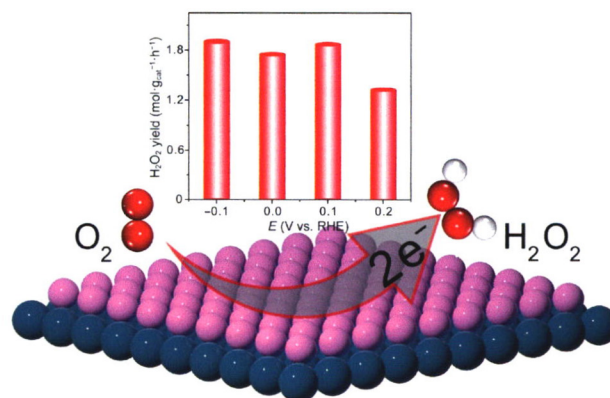
3920–3926

Investigation of MXenes as oxygen reduction electrocatalyst for selective H₂O₂ generation

Xiao Huang¹, Min Song¹, Jian Zhang^{1,*}, Jingjing Zhang¹, Wei Liu¹, Chang Zhang¹, Wang Zhang^{2,*}, and Deli Wang¹

¹ Huazhong University of Science and Technology, China

² Shenzhen University, China



O-terminated MXenes

We found here MXenes are inherent two-electron oxygen reduction reaction (ORR) catalysts. Nb₂CT_x shows a high H₂O₂ production rate of 1.95 mol·g_{cat}⁻¹·h⁻¹ at 0.1 V (vs. reversible hydrogen electrode (RHE)) and can efficiently decompose organic dyes.

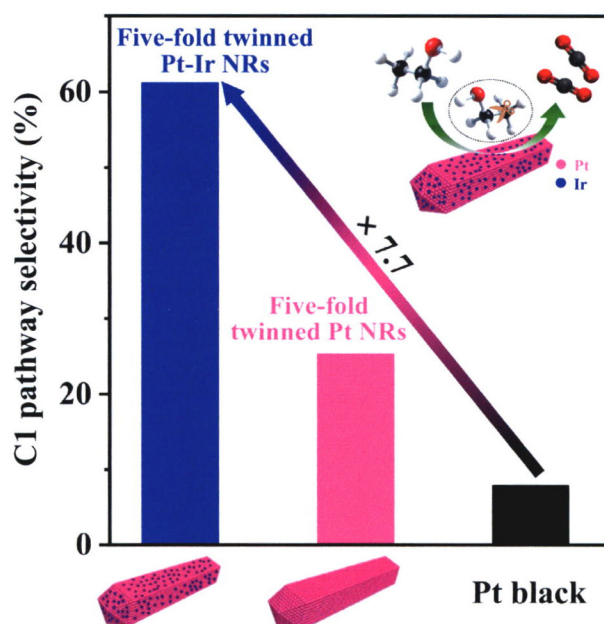
3927–3932

Five-fold twinned Ir-alloyed Pt nanorods with high C1 pathway selectivity for ethanol electrooxidation

Yan Fang¹, Shiyu Guo¹, Dongjie Cao¹, Genlei Zhang^{1,*}, Qi Wang¹, Yazhong Chen¹, Peng Cui¹, Sheng Cheng¹, and Wansheng Zuo²

¹ Hefei University of Technology, China

² Wuhu Tus-semiconductor Co., China



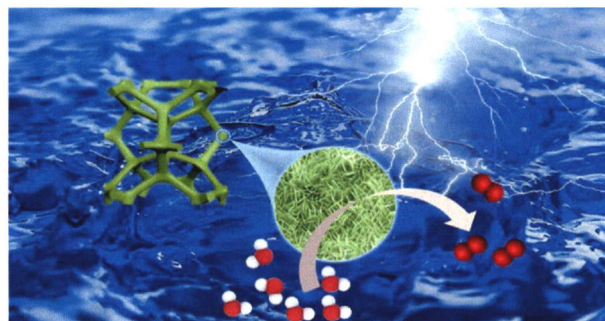
Five-fold twinned (FFT) Pt-Ir nanorods (NRs) are synthesized and exhibit outstanding electrocatalytic performance for ethanol oxidation with a considerable C1 pathway selectivity.

3933–3939

Mn-doping induced electronic modulation and rich oxygen vacancies on vertically grown NiFe₂O₄ nanosheet array for synergistically triggering oxygen evolution reaction

Yonghao Gan, Meilin Cui, Xiaoping Dai^{*}, Ying Ye, Fei Nie, Ziteng Ren, Xueli Yin, Baoqiang Wu, Yihua Cao, Run Cai, and Xin Zhang

China University of Petroleum, China



Mn-doped NiFe₂O₄ induces the electronic modulation to entitle the hybridization between Ni 3d and O 2p orbitals to facilitate the formation of *OOH, and also creates more oxygen vacancies to reduce the adsorption energy of water molecules for triggering OER process.

3940–3945

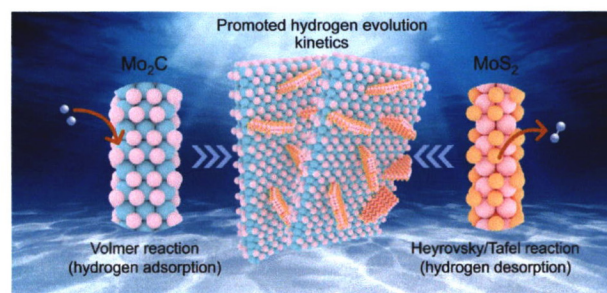
Vertically mounting molybdenum disulfide nanosheets on dimolybdenum carbide nanomeshes enables efficient hydrogen evolution

Tingting Wang¹, Pengyan Wang¹, Yajun Pang^{2,*}, Yitian Wu², Jin Yang², Hao Chen², Xiaorui Gao³, Shichun Mu¹, and Zongkui Kou^{1,*}

¹ Wuhan University of Technology, China

² Zhejiang A&F University, China

³ Changshu Institute of Technology, China



A two-dimensional (2D) layered-nanosheet-on-2D-nonlayered-nanomesh hierarchical heterostructure was fabricated to aim at weakening the strong hydrogen adsorption strength of Mo₂C by introducing the MoS₂ featuring the strong hydrogen intermediate desorption capacity.

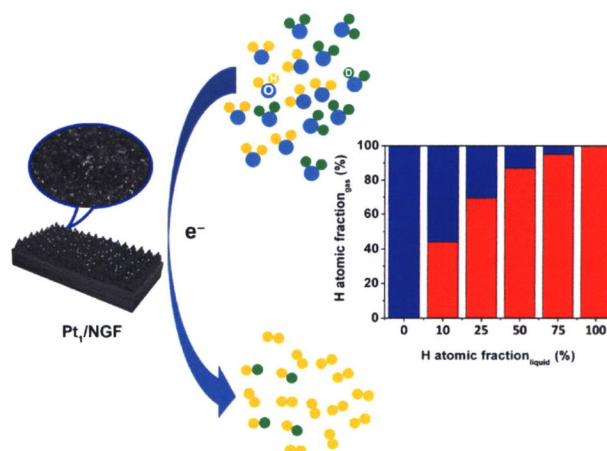
3946–3951

Platinum single atom catalysts for hydrogen isotope separation during hydrogen evolution reaction

Jingsong Xu¹, Rui Li², Xiayan Yan², Qingkai Zhao², Rongguang Zeng², Jingwen Ba², Qifa Pan¹, Xin Xiang^{2,*}, and Daqiao Meng^{1,*}

¹ Science and Technology on Surface Physics and Chemistry Laboratory, China

² Institute of Materials, China Academy of Engineering Physics, China



Pt single atom catalysts (SACs) were anchored on nitrogen doped graphite foil by polyol reduction method. The as-prepared Pt SACs exhibited high activity with an overpotential of 0.022 V at 10 mA·cm⁻² toward hydrogen evolution reaction and a high separation factor of 6.83 toward H/D separation.

3952–3958

Atomically dispersed Ni anchored on polymer-derived mesh-like N-doped carbon nanofibers as an efficient CO₂ electrocatalytic reduction catalyst

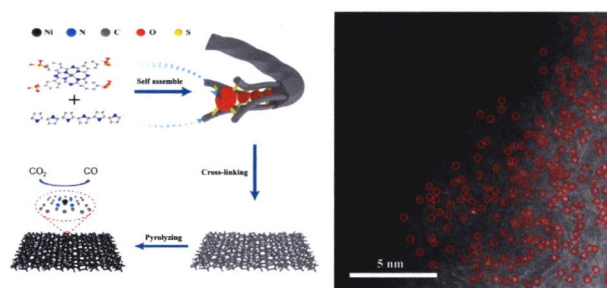
Tai Cao¹, Rui Lin¹, Shoujie Liu², Weng-Chon (Max) Cheong³, Zhi Li^{1,*}, Konglin Wu², Youqi Zhu⁴, Xiaolu Wang¹, Jian Zhang¹, Qiheng Li¹, Xiao Liang¹, Ninghua Fu¹, Chen Chen¹, Dingsheng Wang¹, Qing Peng¹, and Yadong Li^{1,*}

¹ Tsinghua University, China

² Anhui Normal University, China

³ University of Macau, Macao, China

⁴ Beijing Institute of Technology, China



A self-assembly strategy was developed to synthesize a highly efficient CO₂ reduction electrocatalyst with atomically dispersed Ni active centers anchored on polymer-derived mesh-like N-doped carbon nanofibers.

3959–3963

S incorporated RuO₂-based nanorings for active and stable water oxidation in acid

Qing Yao^{1,2}, Zhiyong Yu¹, Ying-Hao Chu³, Yu-Hong Lai³, Ting-Shan Chan⁴, Yong Xu^{5,*}, Qi Shao¹, and Xiaoqing Huang^{2,*}

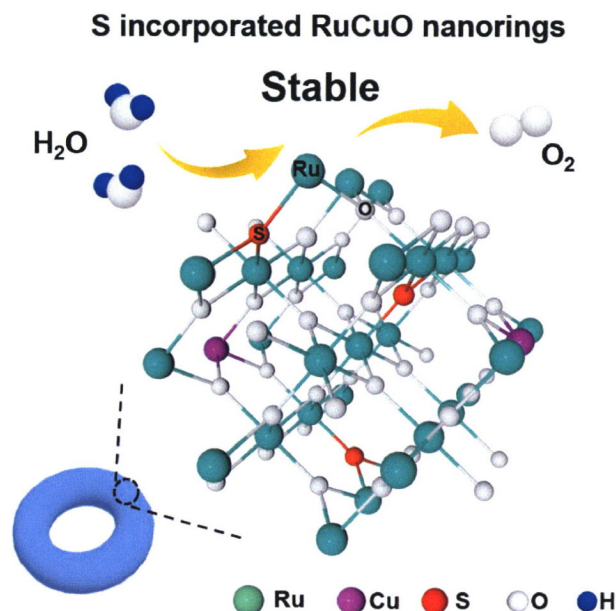
¹ Soochow University, China

² Xiamen University, China

³ "National Yang Ming Chiao Tung University", Taiwan, China

⁴ "National Synchrotron Radiation Research Center", Taiwan, China

⁵ Guangdong University of Technology, China



We demonstrate that the incorporation of S into RuCuO nanorings (NRs) can optimize the interaction of Ru and O and significantly suppresses the dissolution of Ru in acidic condition. The optimal catalyst exhibits enhanced stability for 3,000 cycles of cyclic voltammetry test and more than 250 h chronopotentiometry test at 10 mA·cm⁻² in 0.5 M H₂SO₄.

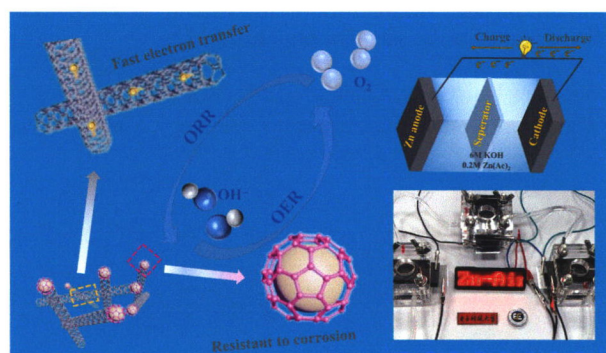
3964–3970

N-doped CNTs capped with carbon layer armored CoFe alloy as highly stable bifunctional catalyst for oxygen electrocatalysis

Bin Wang¹, Katam Srinivas¹, Yanfang Liu¹, Dawei Liu¹, Xiaojuan Zhang¹, Wanli Zhang¹, and Yuanfu Chen^{1,2,*}

¹ University of Electronic Science and Technology of China, China

² Tibet University, China



A bifunctional oxygen evolution reaction (OER)/oxygen reduction reaction (ORR) electrocatalyst with exceptional operating stability was designed to meet the practical application for Zn-air batteries.

3971–3979

Biomass-assisted approach for large-scale construction of multi-functional isolated single-atom site catalysts

Tao Wu^{1,2,3}, Sha Li⁴, Shoujie Liu⁴, Weng-Chon Cheong⁵, Cheng Peng¹, Kai Yao¹, Yingping Li¹, Jieyue Wang¹, Binbin Jiang^{6,*}, Zheng Chen^{3,*}, Zhiming Chen², Xianwen Wei¹, and Konglin Wu^{1,2,*}

¹ Anhui University of Technology, China

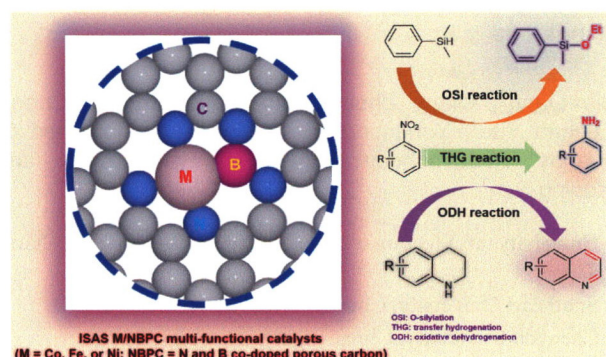
² Anhui Polytechnic University, China

³ Anhui Normal University, China

⁴ Chemistry and Chemical Engineering of Guangdong Laboratory, China

⁵ University of Macau, Macao, China

⁶ Anqing Normal University, China



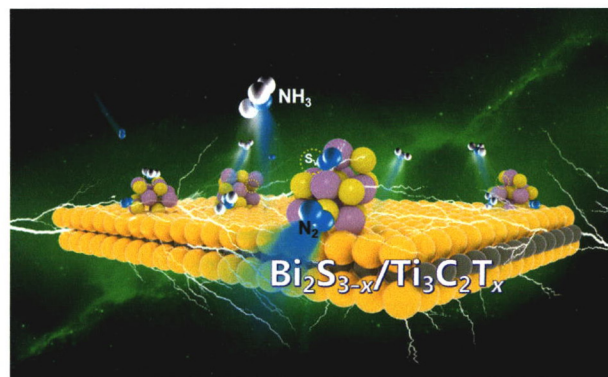
A biomass-assisted pyrolysis-etching-activation (PEA) strategy was developed to construct ISAS metal decorated on N and B co-doped porous carbon (ISAS M/NBPC, M = Co, Fe, or Ni) catalysts with multi-functional features and excellent catalytic activities. They can be used to conduct different types of catalytic reactions, such as O-silylation (OSI), oxidative dehydrogenation (ODH), and transfer hydrogenation (THG).

3980–3990

Sulfur-deficient $\text{Bi}_2\text{S}_{3-x}$ synergistically coupling $\text{Ti}_3\text{C}_2\text{T}_x$ -MXene for boosting electrocatalytic N_2 reduction

Yaojing Luo, Peng Shen, Xingchuan Li, Yali Guo, and Ke Chu

Lanzhou Jiaotong University, China



Sulfur-deficient $\text{Bi}_2\text{S}_{3-x}$ nanoparticles decorated $\text{Ti}_3\text{C}_2\text{T}_x$ -MXene exhibited a dramatically boosted electrocatalytic N_2 reduction activity with an NH_3 yield of $68.3 \mu\text{g}\cdot\text{h}^{-1}\cdot\text{mg}^{-1}$ and a Faradaic efficiency of 22.5%, attributed to the dual-active-centers of S-vacancies and interfacial-Bi sites for strongly boosting N_2 adsorption and $^*\text{N}_2\text{H}$ formation to result in an energetic-favorable nitrogen reduction reaction (NRR) process.

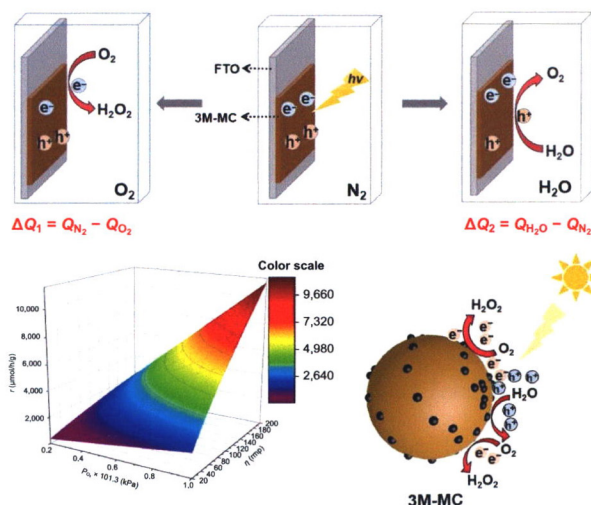
3991–3999

Highly efficient metal-free catalyst from cellulose for hydrogen peroxide photoproduction instructed by machine learning and transient photovoltage technology

Yan Liu¹, Xiao Wang¹, Yajie Zhao¹, Qingyao Wu¹, Haodong Nie¹, Honglin Si¹, Hui Huang^{1,*}, Yang Liu^{1,*}, Mingwang Shao^{1,*}, and Zhenhui Kang^{1,2,*}

¹ Soochow University, China

² Macau University of Science and Technology, Macau, China



Metal-free photocatalyst from cellulose shows the high photocatalytic activity and anti-poisoning properties for the photoproduction of H_2O_2 instructed by transient photovoltage technology and machine learning.

4000–4007

FeP nanorod array: A high-efficiency catalyst for electroreduction of NO to NH_3 under ambient conditions

Jie Liang¹, Qiang Zhou², Ting Mou¹, Hongyu Chen¹, Luchao Yue¹, Yongsong Luo¹, Qian Liu³, Mohamed S. Hamdy⁴, Abdulmohsen Ali Alshehri⁵, Feng Gong^{2,*}, and Xuping Sun^{1,*}

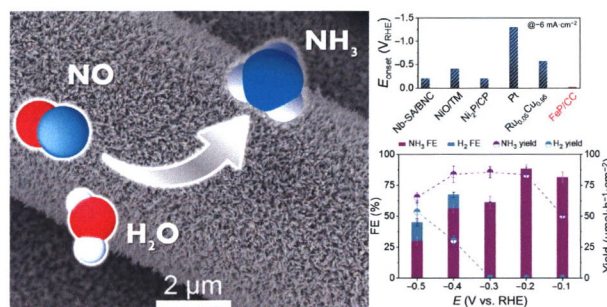
¹ University of Electronic Science and Technology of China, China

² Southeast University, China

³ Chengdu University, China

⁴ King Khalid University, Saudi Arabia

⁵ King Abdulaziz University, Saudi Arabia



An FeP nanorod array supported on carbon cloth (FeP/CC) behaves as a high-active electrocatalyst with a low onset potential toward NO -to- NH_3 conversion, achieving a remarkable Faradaic efficiency of 88.49% and a large yield of $85.62 \mu\text{mol}\cdot\text{h}^{-1}\cdot\text{cm}^{-2}$ in 0.2 M phosphate-buffered solution.

4008–4013

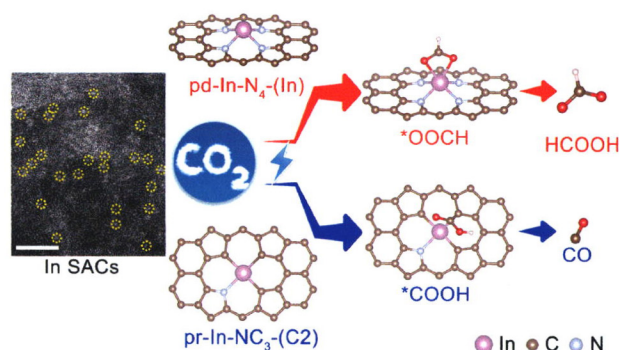
Tuning the reaction path of CO₂ electroreduction reaction on indium single-atom catalyst: Insights into the active sites

Jiawei Zhang¹, Gangming Zeng¹, Lanlan Chen², Wenchuan Lai¹, Yuliang Yuan¹, Yangfan Lu³, Chao Ma¹, Wenhua Zhang^{2,*}, and Hongwen Huang^{1,*}

¹ Hunan University, China

² University of Science and Technology of China, China

³ Zhejiang University, China



Electrochemical CO₂ reduction (CO₂RR) selectivity switch from HCOOH to CO in In single-atom catalysts (SACs) enabled by active sites shift from indium center to the indium-adjacent carbon atoms.

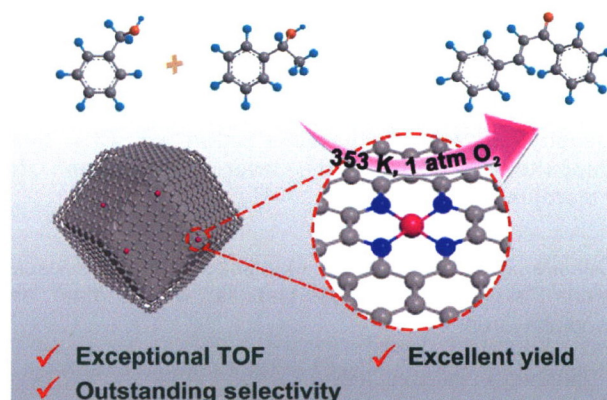
4014–4022

Synthesis of cobalt single atom catalyst by a solid-state transformation strategy for direct C–C cross-coupling of primary and secondary alcohols

Zhijun Li^{1,*}, Yuying Chen¹, Xiaowen Lu¹, Honghong Li¹, Leipeng Leng¹, Tinglei zhang¹, and J. Hugh Horton^{1,2}

¹ Northeast Petroleum University, China

² Queen's University, Canada



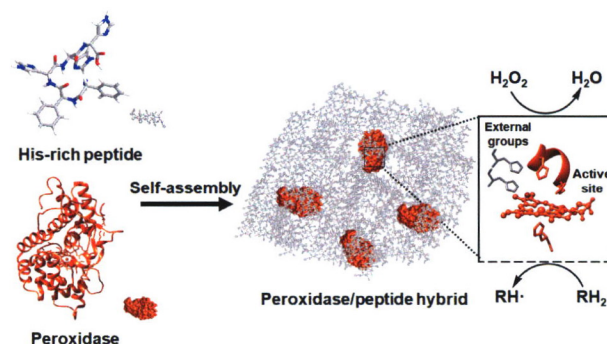
Herein, we report a solid-state transformation strategy to fabricate Co single atom catalysts by introducing Co species from commercial Co₂O₃ powders into nitrogen-doped carbon support. Its exceptional catalytic performance in the direct C–C cross-coupling of primary and secondary alcohols was experimentally validated and further confirmed by density functional theory calculations.

4023–4031

Designed histidine-rich peptide self-assembly for accelerating oxidase-catalyzed reactions

Peidong Du, Siyuan Liu, Hao Sun, Haifeng Wu, and Zhen-Gang Wang

Beijing University of Chemical Technology, China



The histidine-rich peptides self-assemble with peroxidases to form biocatalytic hybrids, in which the histidine from the peptides may collaborate with the residues in the heme pocket of the enzyme to accelerate the catalytic rate toward H₂O₂-oxidation of electron donor substrates.

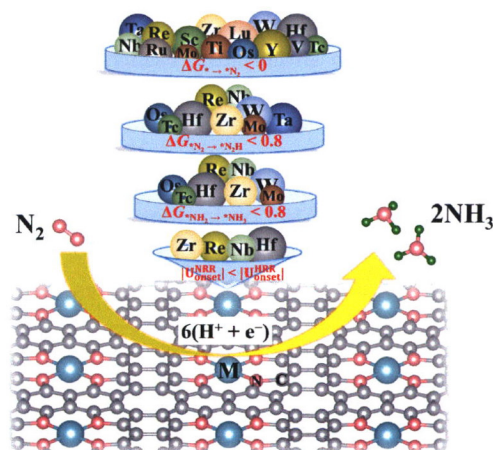
4032–4038

Single-atom catalysts based on two-dimensional metalloporphyrin monolayers for ammonia synthesis under ambient conditions

Chun-Xiang Huang^{1,2}, Sheng-Yao Lv^{1,2}, Cong Li¹, Bin Peng², Guoliang Li^{2,*}, and Li-Ming Yang^{1,*}

¹ Huazhong University of Science and Technology, China

² South China Normal University, China



Four novel metal porphyrin MPP (M = Zr, Nb, Hf and Re) single-atom catalyst candidates with excellent performance for ammonia (NH₃) synthesis from electrocatalytic nitrogen reduction reaction (NRR) have been identified through a combination of four-step high-throughput screening and first-principles calculations on a series of 3d, 4d, and 5d transition metals anchored onto porphyrin substrates.

4039–4047

Energy

Research Articles

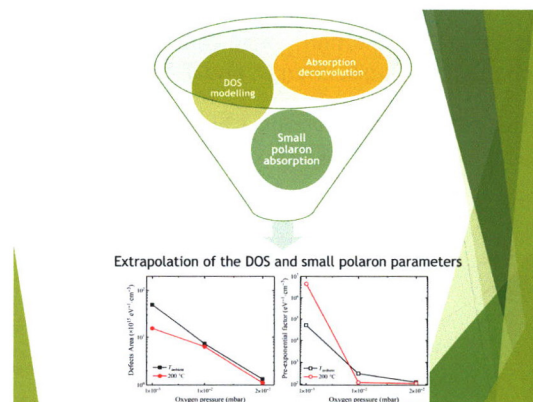
Density of states characterization of TiO₂ films deposited by pulsed laser deposition for heterojunction solar cells

Daniele Scirè^{1,*}, Roberto Macaluso¹, Mauro Mosca¹, Maria Pia Casaletto², Olindo Isabella³, Miro Zeman³, and Isodiana Crupi¹

¹ University of Palermo, Italy

² National Research Council (CNR), Italy

³ Delft University of Technology, the Netherlands



The application of TiO₂ has an important role as electron selective contact in heterojunction technology (HJT), but knowledge of the defect density of states (DOS) is incomplete. We provide the defect density of states and the small polaron parameters after an optical non-destructive characterization.

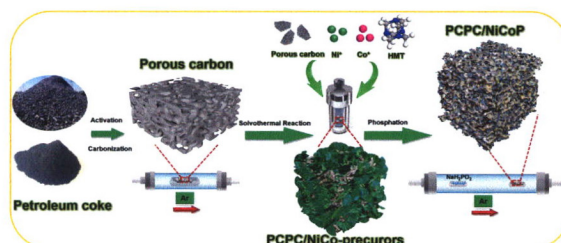
4048–4057

Petroleum coke derived porous carbon/NiCoP with efficient reviving catalytic and adsorptive activity as sulfur host for high performance lithium–sulfur batteries

Bo Zhang¹, Lu Wang¹, Bin Wang¹, Yanjun Zhai², Shuyuan Zeng², Meng Zhang¹, Yitai Qian¹, and Liqiang Xu^{1,*}

¹ Shandong University, China

² Liaocheng University, China



A distinct multifunctional integrated sulfur-host of petroleum coke-based porous carbon/NiCoP composites was prepared for capturing lithium polysulfides (LiPSs) and accelerating the conversion reaction kinetics of LiPSs.

4058–4067

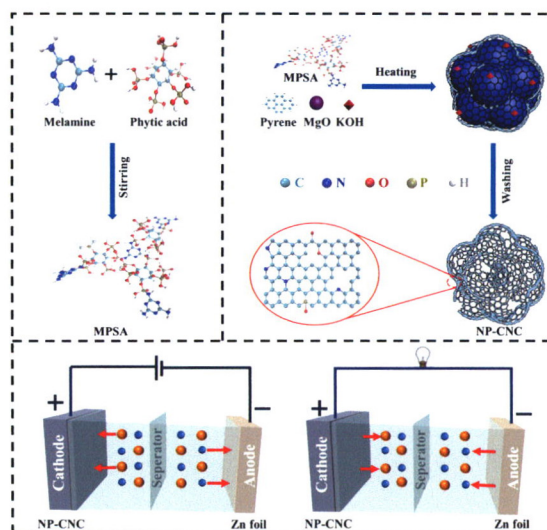
Interconnected N/P co-doped carbon nanocage as high capacitance electrode material for energy storage devices

Lei Yang¹, Xiaojun He^{1,*}, Yuchen Wei¹, Honghui Bi¹, Feng Wei¹, Hongqiang Li¹, Changzhou Yuan^{2,*}, and Jieshan Qiu^{3,*}

¹ Anhui University of Technology, China

² University of Jinan, China

³ Beijing University of Chemical Technology, China



Interconnected N/P co-doped carbon nanocage (NP-CNC) was synthesized from pyrene molecules by using MgO as template and melamine-phytic acid supramolecular aggregate (MPSA) as dopant coupled with KOH activation, presenting outstanding electrochemical properties as electrode material of energy storage devices.

4068–4075

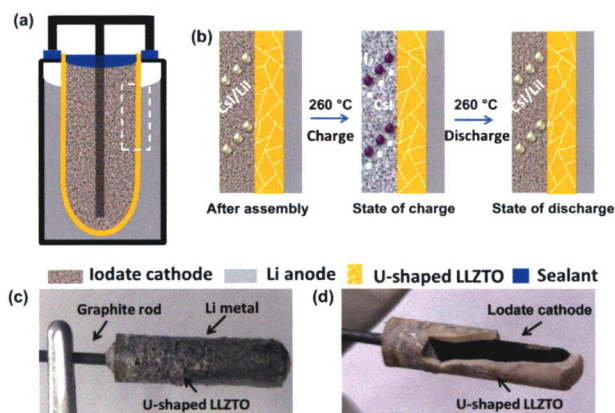
A garnet-electrolyte based molten Li-I₂ battery with high performance

Bin Sun¹, Panpan Wang^{1,2}, Jing Xu¹, Qianzheng Jin^{1,*}, Zili Zhang¹, Hui Wu^{3,*}, and Yang Jin^{1,*}

¹ Zhengzhou University, China

² Xiangtan university, China

³ Tsinghua University, China



Here, we firstly report a molten Li-I₂ battery (MLIB) based on the U-shaped garnet Li_{6.4}La₃Zr_{1.4}Ta_{0.6}O₁₂ (LLZTO) ceramic electrolyte tube at a moderate operating temperature of 260 °C, comprised of a molten lithium anode and a molten CsI/LiI eutectic salt cathode. The high active material LiI loading in a single cell can reach up to 593 mg (~173.7 mg·cm⁻²).

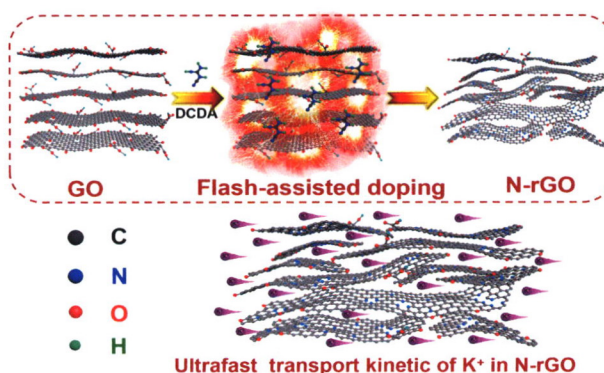
4076–4082

Flash-assisted doping graphene for ultrafast potassium transport

Yongzhi Zhang^{1,2}, Xianjue Chen², Wanglai Cen¹, Wenhao Ren², Haocheng Guo², Sicheng Wu², Yang Xiao², Sheng Chen², Yong Guo², Dan Xiao^{1,*}, and Chuan Zhao^{2,*}

¹ Sichuan University, China

² University of New South Wales, Australia



A flash-assisted doping method was proposed to produce nitrogen- and sulfur-doped graphene (N-rGO and S-rGO). Particularly, the as-synthesized N-rGO with a high N content of 12.75 at.% and abundant structure defects used as potassium ion battery anodes exhibits ultrafast transport kinetics of K⁺.

4083–4090

Stabilizing effects of atomic Ti doping on high-voltage high-nickel layered oxide cathode for lithium-ion rechargeable batteries

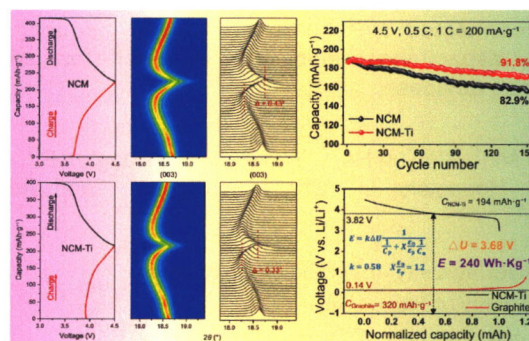
Yong Cheng^{1,2}, Yan Sun³, Changting Chu¹, Limin Chang^{1,*}, Zhaomin Wang³, Dongyu Zhang², Wanqiang Liu^{3,*}, Zechao Zhuang^{4,*}, and Limin Wang^{1,2}

¹ Jilin Normal University, China

² Changchun Institute of Applied Chemistry, Chinese Academy of Sciences, China

³ Changchun University of Science and Technology, China

⁴ Tsinghua University, China



The homogeneous Ti-doped high-voltage high-nickel lithium layered oxide cathode $\text{LiNi}_{0.6}\text{Co}_{0.2}\text{Mn}_{0.18}\text{Ti}_{0.02}\text{O}_2$ (NCM-Ti) is successfully prepared through a liquid phase physical mixing and high-temperature annealing method. Ti doping inhibits the undesired $\text{H}_2\text{-H}_3$ phase transition, minimizing the mechanical degradation due to the strong Ti-O bond and no unpaired electrons for Ti^{4+} , and Ti-doped NCM shows superior cycle stability and an energy density of up to $240 \text{ Wh}\cdot\text{Kg}^{-1}$.

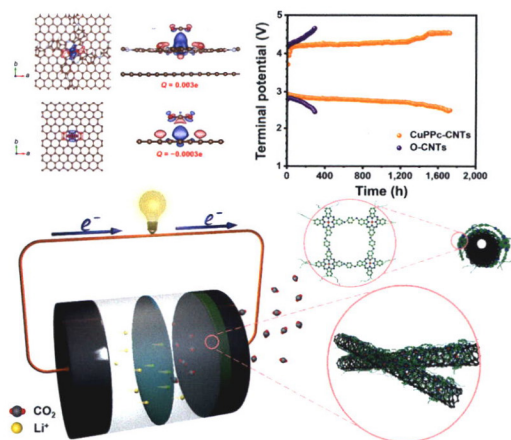
4091–4099

Single atom site conjugated copper polyphthalocyanine assisted carbon nanotubes as cathode for reversible Li-CO_2 batteries

Yunyun Xu¹, Cheng Jiang¹, Hao Gong², Hairong Xue¹, Bin Gao¹, Peng Li¹, Kun Chang¹, Xianli Huang¹, Tao Wang^{1,*}, and Jianping He¹

¹ Nanjing University of Aeronautics and Astronautics, China

² Nanjing Forestry University, China



Conjugated copper polyphthalocyanine significantly improved the CO_2 adsorption and carbon nanotubes have excellent electrical conductivity. The composites (CuPPc-CNTs) provide an opportunity for the research of covalent organic polymers (COPs) single-atom catalyst in Li-CO_2 battery field.

4100–4107

Assembly of flower-like $\text{VS}_2/\text{N-doped}$ porous carbon with expanded (001) plane on rGO for superior Na-ion and K-ion storage

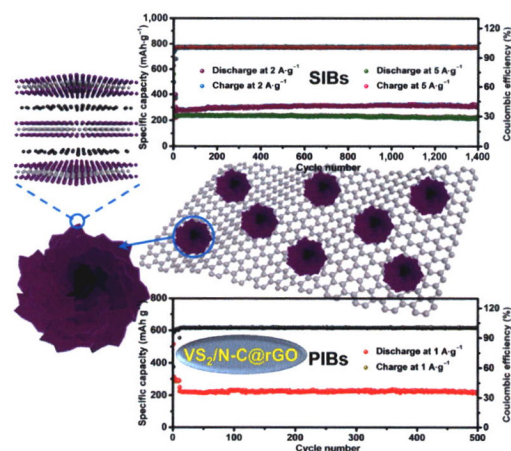
Junwei Sun¹, Gang Lian^{1,*}, Laiying Jing², Di Wu¹, Deliang Cui¹, Qilong Wang³, Haohai Yu^{1,*}, Huaijin Zhang¹, and Ching-Ping Wong⁴

¹ Shandong University, China

² Qilu University of Technology (Shandong Academy of Sciences), China

³ Shandong University, China

⁴ Georgia Institute of Technology, USA



The interlayer-expanded VS_2 nanoflowers via alternated intercalation of N-doped carbon (N-C) monolayers are rationally designed and grown on reduced graphene oxide (rGO). The obtained $\text{VS}_2/\text{N-C}@r\text{GO}$ nanohybrids, as electrode materials for sodium-ion batteries (SIBs) and potassium-ion batteries (PIBs), exhibit excellent electrochemical energy storage performance.

4108–4116

Multishelled CuO/Cu₂O induced fast photo-vapour generation for drinking water

Xuanbo Chen^{1,2}, Ping Li³, Jiao Wang^{2,4}, Jiawei Wan^{2,5}, Nailliang Yang^{2,5,*}, Bo Xu⁶, Lianming Tong⁶, Lin Gu^{5,7}, Jiang Du⁴, Jianjian Lin^{3,*}, Ranbo Yu^{1,*}, and Dan Wang^{2,5,*}

¹ University of Science and Technology Beijing, China

² Chinese Academy of Sciences, China

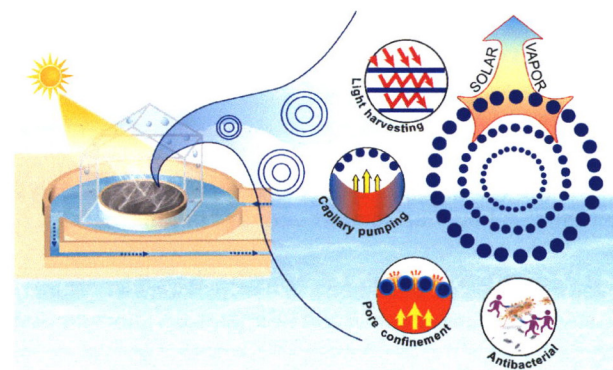
³ Qingdao University of Science and Technology, China

⁴ Zhengzhou University, China

⁵ University of Chinese Academy of Sciences, China

⁶ Peking University, China

⁷ Institute of Physics, Chinese Academy of Sciences, China



Hollow multishelled structure (HoMS) CuO/Cu₂O was introduced into the solar-vapour generation. The porous nano/micro HoMS enhanced light absorption, optimized the thermal regulation and water transport, resulting in a high water evaporation rate, and the heterogeneous semiconductors enhanced the production of reactive oxygen species for water disinfection.

4117–4123

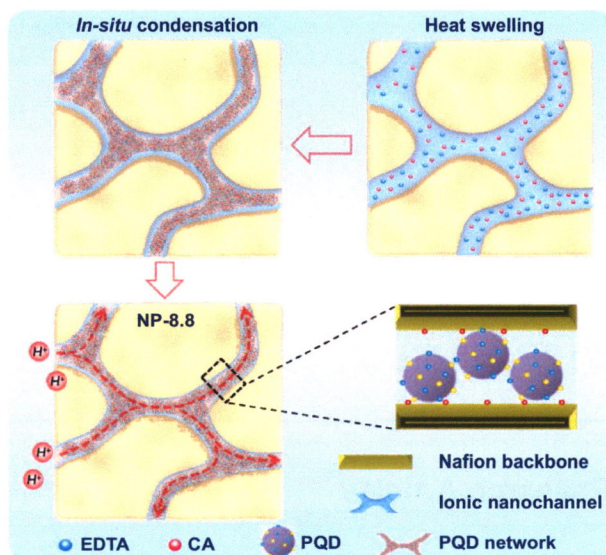
Manipulating the ionic nanophase of Nafion by *in-situ* precise hybridization with polymer quantum dot towards highly enhanced fuel cell performances

Wenjia Wu¹, Zhuofan Zhou¹, Yan Wang¹, Yatao Zhang¹, Yong Wang², Jingtao Wang^{1,*}, and Yecheng Zou³

¹ Zhengzhou University, China

² Nanjing Tech University, China

³ Shandong DongYue Polymer Material Co., Ltd., China



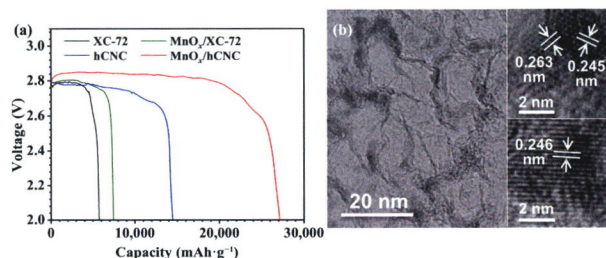
An *in-situ* precise hybridization strategy, mainly containing heat swelling-enabled uniform precursor entrance and microwave-assisted in-situ condensation process, is proposed for decorating Nafion ionic nanochannel. This decoration strategy can precisely manipulate the physical topology and chemical environment of ionic nanochannel without affecting the backbone nanophase function.

4124–4131

Defect-induced deposition of manganese oxides on hierarchical carbon nanocages for high-performance lithium-oxygen batteries

Baoxing Wang, Chenxia Liu, Lijun Yang, Qiang Wu, Xizhang Wang, and Zheng Hu

Nanjing University, China



The MnO_x/hCNC cathode by defect-induced deposition exhibits high full discharge capacity and superior cycle life for Li-O₂ batteries, owing to the boosted reversibility of oxygen reactions by the highly dispersed MnO_x nanoparticles and the fast charge/mass transfer facilitated by the hierarchical carbon nanocages (hCNC).

4132–4136

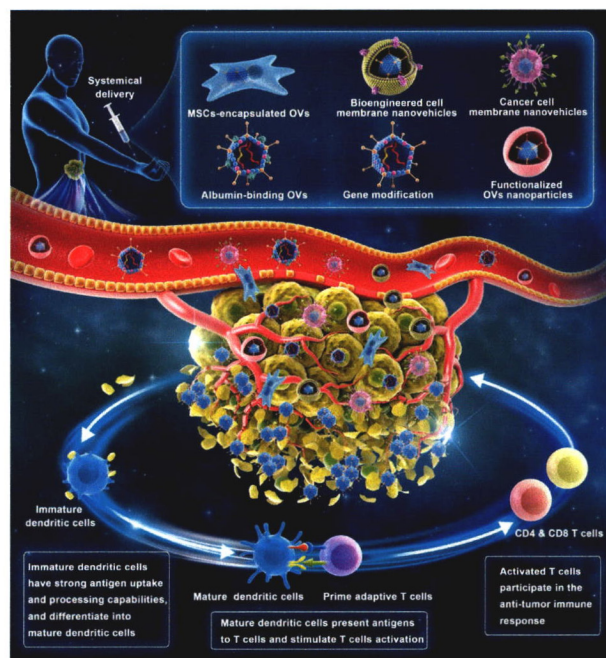
Review Article

Emerging systemic delivery strategies of oncolytic viruses: A key step toward cancer immunotherapy

Weiyue Ban¹, Jianhuan Guan¹, Hanwei Huang²,
Zhonggui He¹, Mengchi Sun^{1,*}, Funan Liu^{2,*}, and Jin Sun¹

¹ Shenyang Pharmaceutical University, China

² China Medical University, China



This abstract graphic takes concerted action with abstract section and illustrates the development status of oncolytic viruses (OVs) systemic delivery modalities. Concretely, six representative systemic delivery models have been exhibited and the physiological disposition and influence for tumor immune microenvironment of OV have been shown in this graphic.

4137–4153

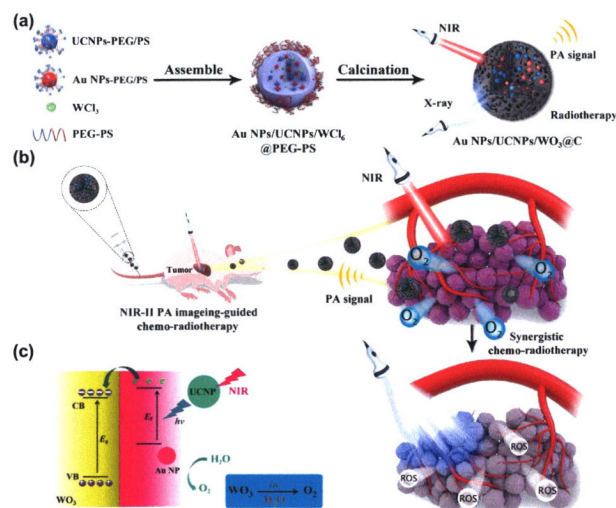
Research Articles

Mesoporous radiosensitized nanoprobe for enhanced NIR-II photoacoustic imaging-guided accurate radio-chemotherapy

Tao Chen¹, Lichao Su¹, Lisen Lin¹, Xiaoguang Ge¹,
Feicheng Bai¹, Meng Niu¹, Chenlu Wang¹, Jibin Song¹,
Shaolei Guo^{2,*}, and Huanghao Yang^{1,*}

¹ Fuzhou University, China

² The First Affiliated Hospital of Sun Yat-Sen University, China



As showed in schematic illustration, we synthesized the WO_3 -based nanoprobe ($\text{Au NPs/UCNPs/WO}_3\text{@C}$) as a smart theranostic agent with the excellent electron excitation and transfer scenarios capability for near-infrared (NIR-II) photoacoustic imaging guided accurate cancer chemo-radiotherapy, which can produce oxygen under radiation and achieve the goal of the hypoxia alleviation in tumor region.

4154–4163

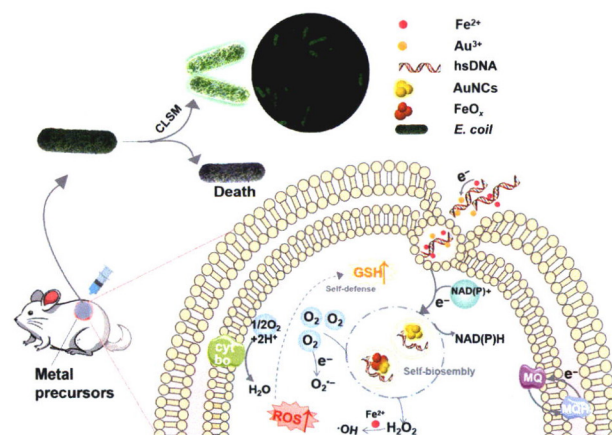
Intelligent bio-assembly imaging-guided platform for real-time bacteria sterilizing and infectious therapy

Jiayu Zeng¹, Zengchao Guo¹, Yihan Wang¹, Zhaojian Qin¹, Yi Ma³, Hui Jiang¹, Yossi Weizmann^{2,*}, and Xuemei Wang^{1,*}

¹ Southeast University, China

² Ben-Gurion University of the Negev, Israel

³ China Pharmaceutical University, China



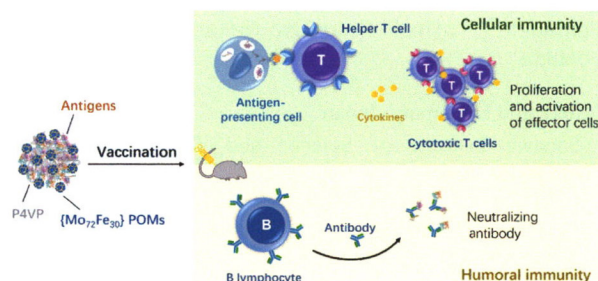
The scheme illustrates the microenvironment-responsive assembled nanoclusters for real-time *Escherichia coli* bioimaging and simultaneous *E. coli*-infected wound cure. In bacterial infections, the metal precursors (i.e., HAuCl_4 , FeCl_2 , and herring sperm DNA) could be bio-self-assembled to multifunctional nanoclusters (NCs) that exhibit luminescence, in which AuCl_4^- was biosynthesized via reductive biomolecules such as NADPH to the fluorescent AuNCs. While visualizing the bacteria, the microenvironment-responsive NCs were enabled to sterilize bacteria efficiently due to reactive oxygen species (ROS) accumulation. Besides, the bio-responsive self-assembled NCs complexes contributed to accelerating bacteria-infected wound healing.

4164–4174

A polymeric co-assembly of subunit vaccine with polyoxometalates induces enhanced immune responses

Xinpei Li, Xiaofeng He, Dongrong He, Yuan Liu, Kun Chen^{*}, and Panchao Yin^{*}

South China University of Technology, China



Supra-particle assemblies are co-assembled by poly(4-vinylpyridine), 2.5 nm iron/molybdenum oxide clusters ($\{\text{Mo}_{72}\text{Fe}_{30}\}$), and antigens of *Mycobacterium bovis* to enhance the vaccine immune response in mice. $\{\text{Mo}_{72}\text{Fe}_{30}\}$ and poly(4-vinylpyridine) together act as vaccine adjuvants that improve the magnitude and durability of antibody responses as well as the T cell-derived cytokine patterns, resulting in enhanced humoral and cellular immune responses.

4175–4180

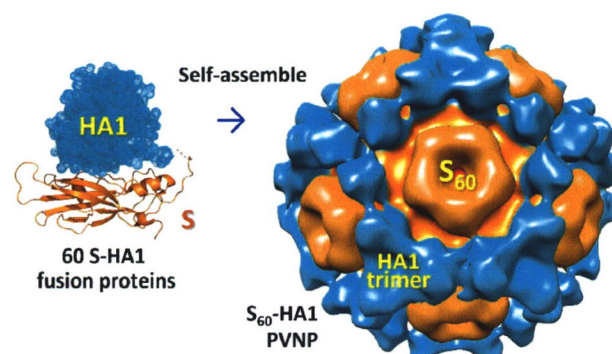
Bioengineered pseudovirus nanoparticles displaying the HA1 antigens of influenza viruses for enhanced immunogenicity

Ming Xia¹, Md Rejaul Hoq², Pengwei Huang¹, Wen Jiang², Xi Jiang^{1,3}, and Ming Tan^{1,3,*}

¹ Cincinnati Children's Hospital Medical Center, USA

² Purdue University, USA

³ University of Cincinnati College of Medicine, USA



A new technology has been developed to generate unique S60-HA1 pseudovirus nanoparticles (PVNPs) that display the receptor-binding HA1 antigens of influenza viruses (IVs). These PVNPs offer new reagents for IV study and provide a promising flu vaccine candidate to fight the deadly influenza.

4181–4190

万方数据

A chitosan-mediated inhalable nanovaccine against SARS-CoV-2

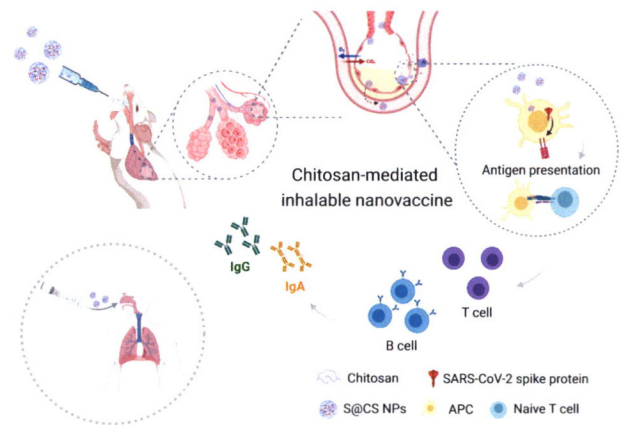
Shao-Hua Zhuo¹, Jun-Jun Wu¹, Lang Zhao¹, Wen-Hao Li¹, Yu-Fen Zhao^{1,4}, and Yan-Mei Li^{1,2,3,*}

¹ Tsinghua University, China

² Beijing Institute for Brain Disorders, China

³ Tsinghua University, China

⁴ Institute of Drug Discovery Technology, Ningbo University, Ningbo 315221, China



The chitosan-mediated inhalable nanovaccine amplifies spike protein immunogenicity, which offers a convenient and compliant strategy to reduce the use of needles and the need for medical staff.

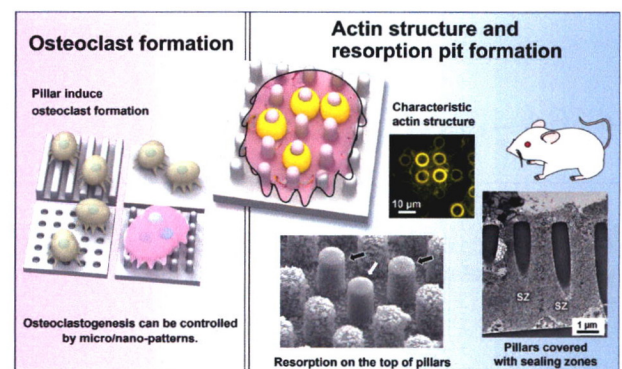
4191–4200

Different micro/nano-scale patterns of surface materials influence osteoclastogenesis and actin structure

Tsukasa Akasaka^{1,*}, Miho Tamai², Yoshitaka Yoshimura¹, Natsumi Ushijima¹, Shinichiro Numamoto¹, Atsuro Yokoyama¹, Hirofumi Miyaji¹, Ryo Takata¹, Shuichi Yamagata¹, Yoshiaki Sato¹, Ko Nakanishi¹, and Yasuhiro Yoshida¹

¹ Hokkaido University, Japan

² Okinawa Institute of Science and Technology Graduate University, Japan



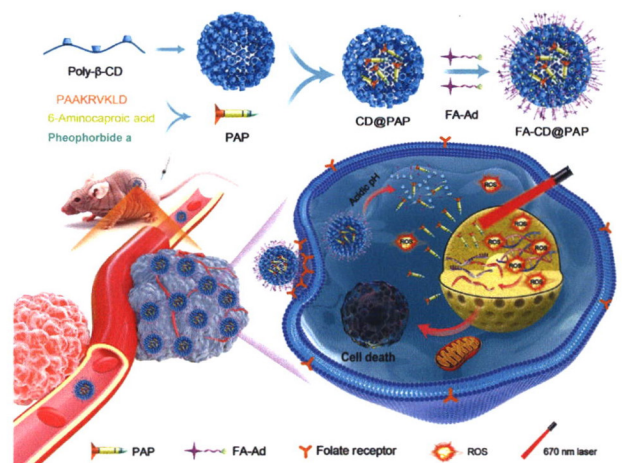
Optimal surface patterns for inducing osteoclastogenesis and characteristic actin structures on pillars were found.

4201–4211

A novel hierarchical targeting and controllable smart nanoparticles for enhanced *in situ* nuclear photodynamic therapy

Gankun Yuan, Qilu Wang, Zifan You, Xuening Chen, Jinping Xue, Xiao Jia^{*}, and Juanjuan Chen^{*}

Fuzhou University, China



The prepared FA-CD@PAP nanoparticles (NPs) can specifically bind to folate receptors (FR)-overexpressed tumor tissues and cells, and decompose the tumor acidic environment to release the nuclear localization signal (NLS) peptide-conjugated photosensitizer PAP (PAP = pyropheophorbide a—PAAKRVKLD), leading to the enhanced nuclear accumulation. DNA could be damaged directly and instantaneously by the reactive oxygen species (ROS) generated inside nuclei for remarkably enhanced cell death.

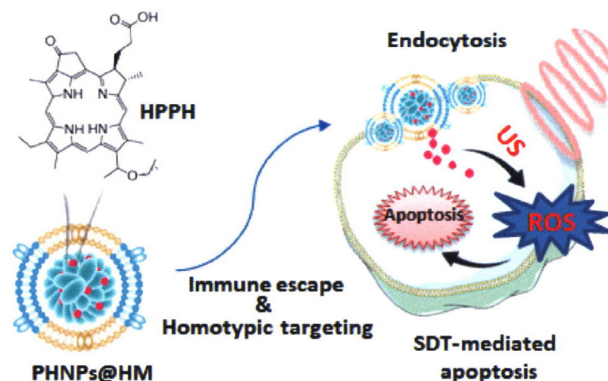
4212–4223

Cancer-macrophage hybrid membrane-camouflaged photochlor for enhanced sonodynamic therapy against triple-negative breast cancer

Lishan Zhang^{1,2}, Ting Yin^{1,2}, Baozhen Zhang², Chong Yan¹, Chengyu Lu¹, Lanlan Liu², Ze Chen², Hui Ran^{1,2}, Qingxia Shi^{1,2}, Hong Pan^{2,*}, Aiqing Ma^{1,2,*}, and Lintao Cai^{2,*}

¹ Guangdong Medical University, China

² Shenzhen Institute of Advanced Technology (SIAT), Chinese Academy of Sciences, China



A 4T1 cancer cell-macrophage hybrid membrane (HM)-camouflaged sonosensitizer nanoplateform is constructed by encapsulating photochlor (HPPH)-loaded albumin nanoparticles (PHNPs). Through homologous adhesion recognition and immune escaping from hybrid membrane, HPPH can be efficiently targeted to the tumor cells and generate reactive oxygen species (ROS) for tumor suppression under ultrasound (US) irradiation.

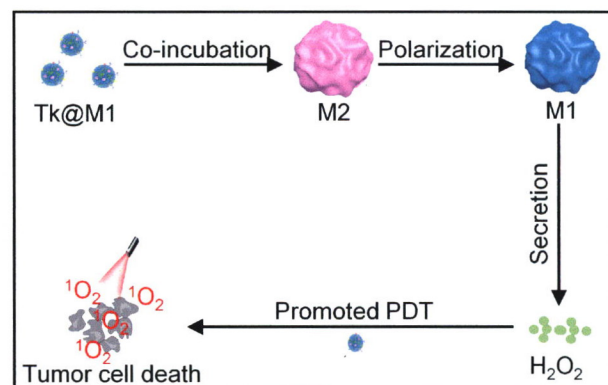
4224–4232

Immunomodulatory hybrid bio-nanovesicle for self-promoted photodynamic therapy

Houli Liu¹, Yao Lei¹, Weidong Nie¹, Helin Zhao¹, Yuzhu Wu¹, Liping Zuo¹, Guanghao Wu¹, Ruili Yang^{2,*}, and Hai-Yan Xie^{1,*}

¹ Beijing Institute of Technology, China

² Peking University, China



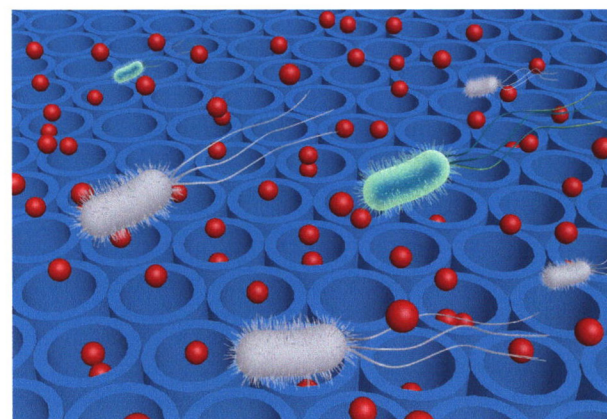
Hybrid bio-nanovesicles (Tk@M1) of thylakoid membranes and M1-macrophage derived extracellular vesicles actively target tumors, and then regulate the inactive tumor immune microenvironment by means of the native features of M1 EV and Tk. The activated tumors promote the photodynamic therapy effect of Tk@M1 attributed to the increased O_2 from catalase catalyzed decomposition of augmented H_2O_2 .

4233–4242

An implantable antibacterial drug-carrier: Mesoporous silica coatings with size-tunable vertical mesochannels

Mengli Liu, Fang Huang, Chin-Te Hung, Liwei Wang, Wei Bi^{*}, Yupu Liu, and Wei Li^{*}

Fudan University, China



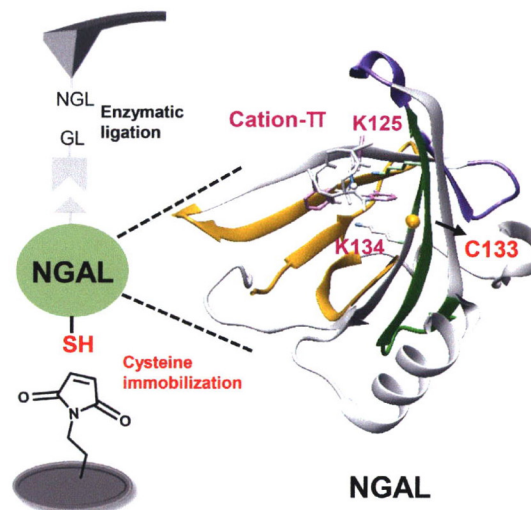
Mesoporous silica coatings (MSCs) with vertical and size-tunable mesochannels are fabricated on a variety of metal substrates via a nano-interfacial oriented assembly approach. Importantly, the MSCs on titanium substrates (Ti@MSCs) exhibit excellent drug adsorption, sustained release, and antibacterial performances.

4243–4250

Detection of weak non-covalent cation- π interactions in NGAL by single-molecule force spectroscopy

Jingyuan Nie, Yibing Deng, Fang Tian, Shengchao Shi, and Peng Zheng*

Nanjing University, China



Cation- π interaction played an essential role in many biological systems. Here, we detected weak influences of cation- π interaction experimentally combining high-precision atomic force microscopy-based single-molecule force spectroscopy (AFM-SMFS) and cysteine-mediated site-specific protein immobilization.

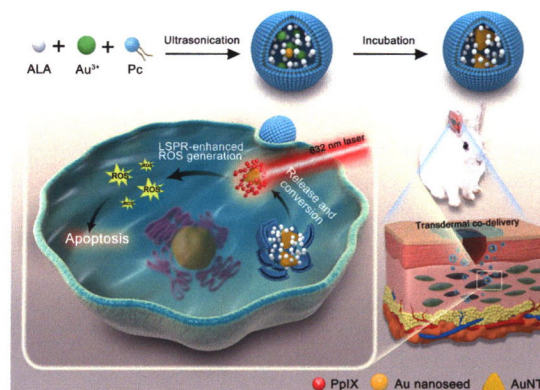
4251–4257

Localized surface plasmon resonance improves transdermal photodynamic therapy of hypertrophic scars

Yunsheng Chen¹, Zhixi Yu¹, Xinxian Meng¹, Hua Li¹, Xiyang Sun^{1,*}, Dannong He², Yixin Zhang^{1,2,*}, and Zheng Zhang^{1,*}

¹ Shanghai Jiao Tong University, China

² Shanghai National Engineering Research Center for Nanotechnology, China



5-Aminolevulinic acid (ALA) and Au nanotriangles (AuNTs) co-delivery nanoethosomes (A/A-ES) achieve the transdermal co-delivery of ALA and AuNTs, and enhance ALA excitation via localized surface plasmon resonance (LSPR) effect. This work provides an effective strategy to improve transdermal photodynamic therapy (PDT) efficacy through LSPR-enhanced reactive oxygen species (ROS) generation

4258–4265

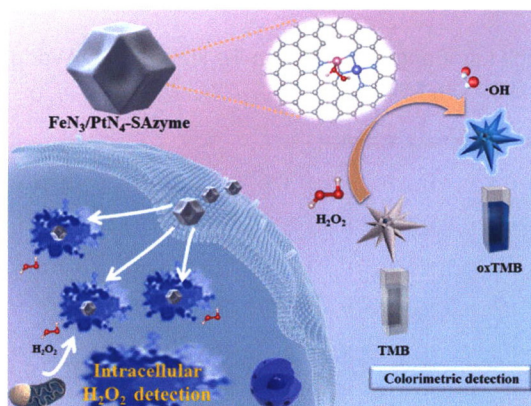
Diatomic active sites nanozymes: Enhanced peroxidase-like activity for dopamine and intracellular H₂O₂ detection

Shan Wang^{1,2}, Zunfu Hu^{1,3,*}, Qiulian Wei^{1,2}, Huimin Zhang¹, Weina Tang¹, Yunqiang Sun¹, Haiqiang Duan¹, Zhichao Dai¹, Qingyun Liu², and Xiuwen Zheng^{1,*}

¹ Linyi University, China

² Shandong University of Science and Technology, China

³ Linyi University, China



A highly efficient single atom nanozymes (FeN₃/PtN₄-SAzyme) with isolated Fe-Pt pairs was presented. With enhanced peroxidase-like activity, FeN₃/PtN₄-SAzyme could apply for colorimetric detection of dopamine and *in-situ* detection of intracellular H₂O₂.

4266–4273

A pH-responsive biomimetic drug delivery nanosystem for targeted chemo-photothermal therapy of tumors

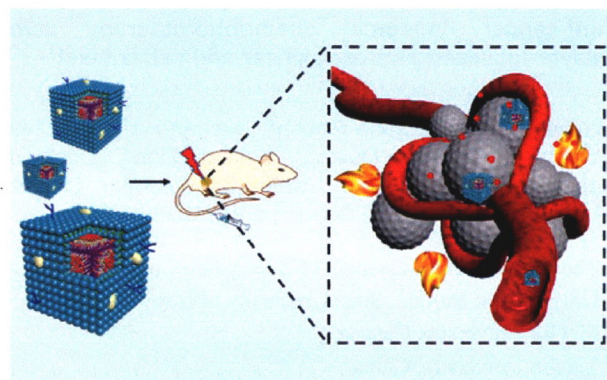
Yanmin Ju^{1,2}, Zhiyi Wang¹, Zeeshan Ali¹, Hongchen Zhang¹, Yazhou Wang¹, Nuo Xu³, Hui Yin⁴, Fugeng Sheng⁴, and Yanglong Hou^{1,*}

¹ Peking University, China

² China Pharmaceutical University, China

³ Fifth Medical Center of Chinese PLA General Hospital, China

4274–4284



A pH-responsive and biomimetic drug delivery nanosystem MnFe₂O₄-DOX-MCM is developed for cancer treatment, which is capability of tumor targeting, pH-stimuli drug release, and chemo-photothermal therapeutic effects.

Indocyanine green assembled free oxygen-nanobubbles towards enhanced near-infrared induced photodynamic therapy

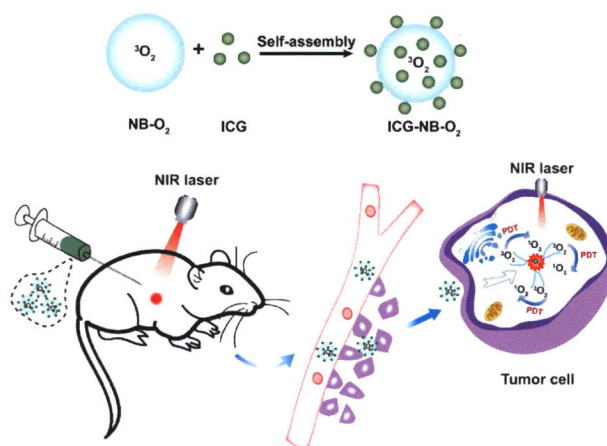
Li Yang¹, Bin Huang^{1,2,*}, Shiqi Hu³, Yuan An¹, Jingyi Sheng¹, Yan Li¹, Yuxin Wang³, and Ning Gu^{1,*}

¹ Southeast University, China

² Jiangsu Second Normal University, China

³ Nanjing Stomatology Hospital, China

4285–4293

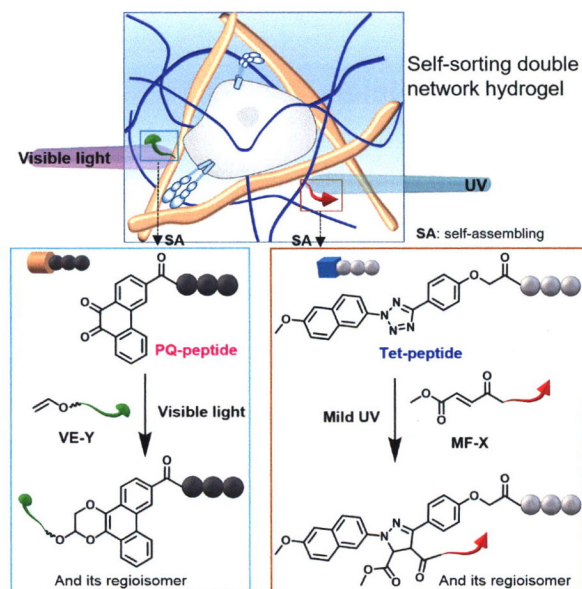


A facile route was developed to fabricate ICG-NBs-O₂ by assembling ICG molecules with free oxygen nanobubbles (NBs-O₂) for enhanced photodynamic therapy (PDT) of oral cancer.

Self-sorting double network hydrogels with photo-definable biochemical cues as artificial synthetic extracellular matrix

Dongdong Wu, Hai Lei, Xian Xie, Liang Zhou, Peng Zheng, Yi Cao^{*}, and Yan Zhang^{*}

Nanjing University, China



Combining peptide self-assembly and photo-click chemistry, a self-sorting double network hydrogel (SDNH) with spatially well-defined bioactive ligands was developed. The programmed SDNH with a desired function through photo-click reactions can be used for a variety of applications such as stem cell culture in 3D.

4294–4301

Anti-cancer liposomal chemophototherapy using bilayer-localized photosensitizer and cabazitaxel

Boyang Sun^{1,2}, Sanjana Ghosh², Xuedan He², Wei-Chiao Huang², Breandan Quinn², Meiling Tian¹, Dushyant Jahagirdar³, Moustafa T. Mabrouk², Joaquin Ortega³, Yumiao Zhang^{4,*}, Shuai Shao^{1,*}, and Jonathan F. Lovell^{2,*}

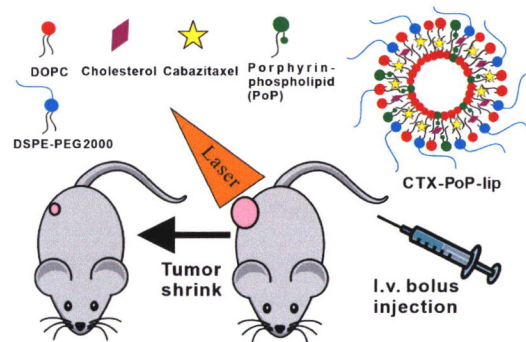
¹ The First Affiliated Hospital of Zhengzhou University, China

² University at Buffalo, State University of New York, USA

³ McGill University, Canada

⁴ Tianjin University, China

4302–4309



Cabazitaxel was loaded into the bilayer of porphyrin-phospholipid (PoP) liposomes and demonstrated synergy for combination chemotherapy and photodynamic therapy.

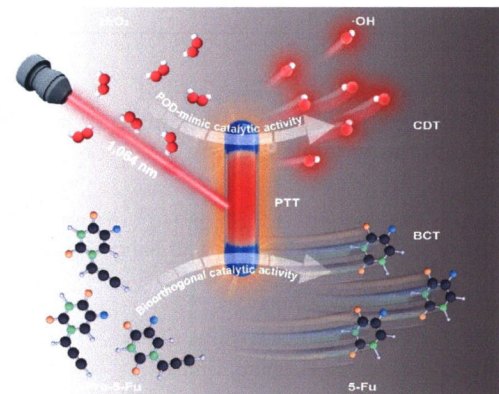
NIR-II photothermal therapy for effective tumor eradication enhanced by heterogeneous nanorods with dual catalytic activities

Linghua Zhang¹, Wenjie Wang¹, Meng Ou¹, Xiaoxiao Huang², Yu Ma¹, Jiayue Tang¹, Ting Hou¹, Sheng Zhang¹, Li Yin¹, Huan Chen¹, Yanglong Hou^{2,*}, and Ya Ding^{1,*}

¹ China Pharmaceutical University, China

² Peking University, China

4310–4319



We successfully design and synthesize bovine serum albumin-coated heterogeneous Pd-Au nanorods to solve the current bottleneck problems of photothermal thermal therapy, and completely eliminate tumors in animal models without toxic side effects by collaborating with heterogeneous nanorod-mediated bioorthogonal catalytic therapy and chemodynamic therapy.

Nano detection

Research Articles

Dynamical investigation of tunable magnetism in Au@Ni-carbide nanocrystals by a combined soft and hard X-ray absorption spectroscopy

Weifeng Huang², Jianxin Kang³, Tingwen Chen³, Dawei Pang⁴, Lihua Wang⁴, Hang Wei^{1,*}, Changchun Yang², Dongfeng Zhang^{3,*}, and Lin Guo^{3,*}

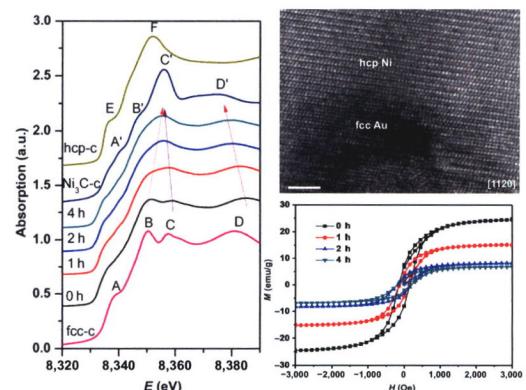
¹ Inner Mongolia University, China

² Jiujiang University, China

³ Beihang University, China

⁴ Beijing University of Technology, China

4320–4326



A series of Au@Ni-carbide magnetic materials are achieved from the controlled carbonation of Au@Ni core-shell structures. Hard X-ray absorption spectroscopy (XAS) at the metal K edge and soft XAS at both metal L edge and carbon K edge provide solid evidence for the carbonation process from fcc-Ni (fcc = face centered cubic) to Ni₃C, rather than phase transformation to hcp-Ni (hcp = hexagonal close packed).

Modulation of electronic state in copper-intercalated 1T-TaS₂

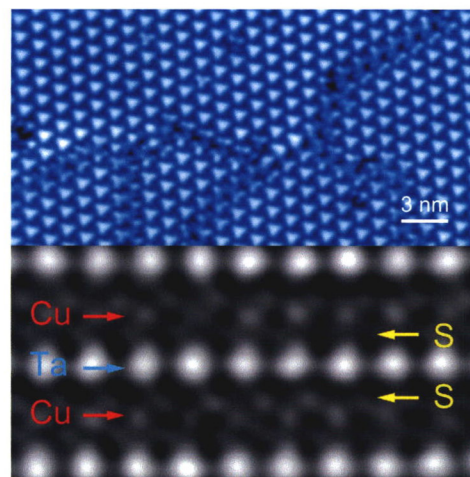
Wenhao Zhang¹, Degong Ding¹, Jingjing Gao², Kunliang Bu¹, Zongxiu Wu¹, Li Wang³, Fangsen Li², Wei Wang², Xuan Luo², Wenjian Lu², Chuanhong Jin^{1,*}, Yuping Sun^{2,4}, and Yi Yin^{1,4,*}

¹ Zhejiang University, China

² Hefei Institutes of Physical Science, Chinese Academy of Sciences, China

³ Suzhou Institute of Nano-Tech and Nano-Bionics, Chinese Academy of Sciences, China

⁴ Nanjing University, China



We characterized the structural and electronic modification of 1T-TaS₂ after Cu intercalation. Novel spatial electronic distributions have been identified in different domains, demonstrating the enhancement of interaction between the star of Davids (SDs) due to the interlayer Cu atoms.

4327–4333

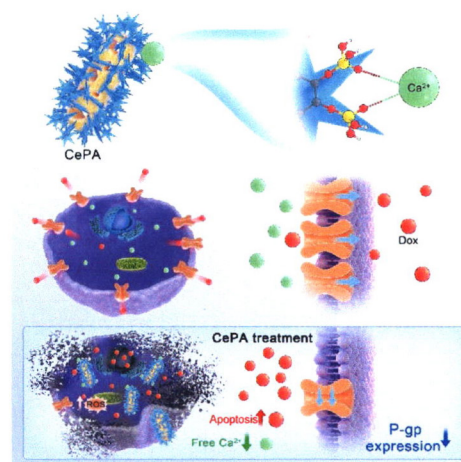
Phytic acid-modified CeO₂ as Ca²⁺ inhibitor for a security reversal of tumor drug resistance

Zhimin Tian¹, Junlong Zhao², Shoujie Zhao², Huicheng Li², Zhixiong Guo¹, Zechen Liang¹, Jiayuan Li¹, Yongquan Qu^{1,*}, Dongfeng Chen^{3,*}, and Lei Liu³

¹ Northwestern Polytechnical University, China

² Fourth Military Medical University, China

³ Army Medical University, China



The Ca²⁺ negative regulation strategy of phytic acid (PA) modified nanoceria has been designed to successfully reverse tumor drug resistance and prevent from doxorubicin (Dox)-induced organ damage. The nano-inhibitor effectively deprives the intracellular excess free Ca²⁺, along with subsequent downregulation of P-glycoprotein (P-gp), and thereby enhances the intracellular drug accumulation in the drug-resistant tumor cells, leading to the improved efficacy of chemotherapeutic agents.

4334–4343

Investigation on the intrinsic wetting thresholds of liquids by measuring the interaction forces of self-assembled monolayers

Yulong Li^{1,2}, Shaofan He^{1,2}, Zhe Xu³, Zhonglong Luo⁴, Hongyan Xiao¹, Ye Tian^{1,2,5,*}, and Lei Jiang^{1,2}

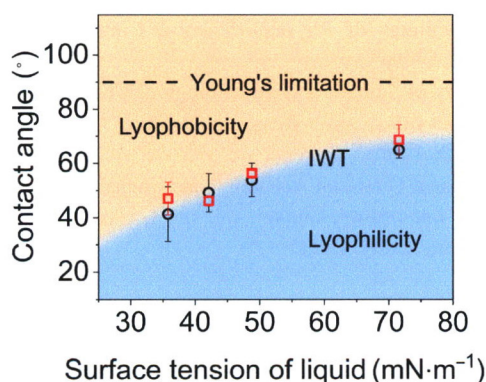
¹ Technical Institute of Physics and Chemistry, Chinese Academy of Sciences, China

² University of Chinese Academy of Sciences, China

³ Beihang University, China

⁴ Anhui University of Technology, China

⁵ Ji Hua Laboratory, China



The intrinsic wetting thresholds (IWTs) of liquids were redefined from the perspective of interaction forces between self-assembled monolayers, which differed from 90° defined by Young's equation.

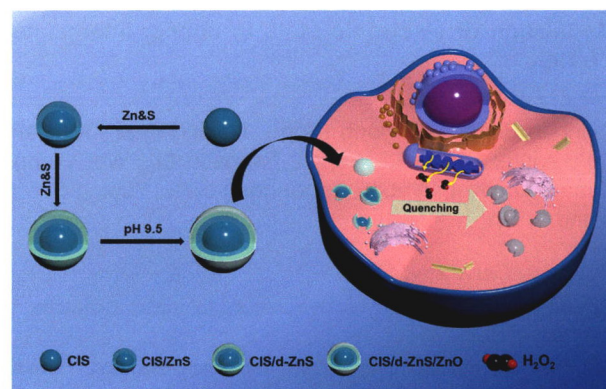
4344–4349

Ultrasensitive determination of intracellular hydrogen peroxide by equipping quantum dots with a sensing layer via self-passivation

Xixi Hu¹, Jia Liu¹, Haozhe Jin¹, Fei Huang¹, Zhaoyin Wang^{1,*}, Fang Wang², and Zhihui Dai^{1,2,*}

¹ Nanjing Normal University, China

² Nanjing Normal University Center for Analysis and Testing, China



Self-passivation of CuInS₂-based quantum dots (QDs) is achieved in a simple one-step process, resulting in the spontaneous and rapid formation of ZnO shells outside of CuInS₂-based QDs. The ZnO shell, serving as a sensing layer, enables sensitive visualization of intracellular hydrogen peroxide generated by mitochondria.

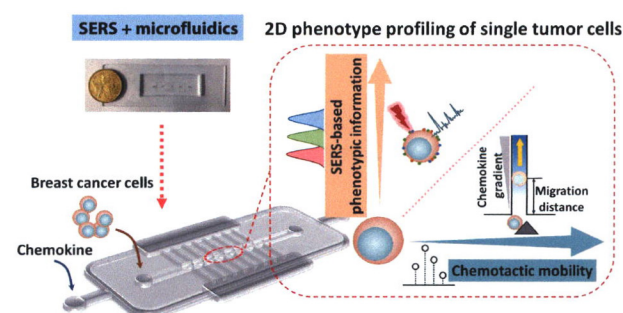
4350–4356

2D profiling of tumor chemotactic and molecular phenotype at single cell resolution using a SERS-microfluidic chip

Yizhi Zhang^{1,2}, Lei Wu¹, Kuo Yang¹, Shenfei Zong¹, Zhuyuan Wang^{1,*}, and Yiping Cui^{1,*}

¹ Southeast University, China

² Nanjing University of Aeronautics and Astronautics, China



A surface enhanced Raman scattering (SERS)-microfluidic chip has been developed for two-dimensional (2D) profiling of tumor chemotactic and molecular phenotype at single-cell resolution.

4357–4365

Nonlinear electronic and ultrafast optical signatures in chemical vapor-deposited ultrathin PtS₂ ribbons

Shaolong Jiang^{1,*}, Jin Yang^{2,3}, Liang Zhu¹, Jiafeng Xie⁴, Weiteng Guo¹, Erding Zhao¹, Chaoyu Chen^{1,5}, Tianwu Wang⁴, Fuhai Su^{2,*}, Yanfeng Zhang^{6,*}, and Junhao Lin^{1,*}

¹ Southern University of Science and Technology, China

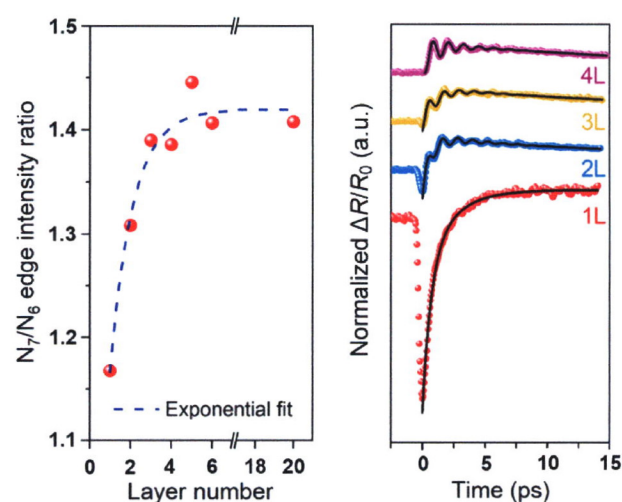
² Hefei Institutes of Physical Science, Chinese Academy of Sciences, China

³ University of Science and Technology of China, China

⁴ Aerospace Information Research Institute, Chinese Academy of Science, China

⁵ International Quantum Academy, and Shenzhen Branch, Hefei National Laboratory, China

⁶ Peking University, China



Ultrathin 1T-PtS₂ ribbons with thickness centralized almost at 1L–4L and large domain size up to 210 μm are synthesized on Au foils using chemical vapor deposition (CVD) technique. The electron and optical absorption properties of PtS₂ are investigated using electron energy loss spectroscopy (EELS) and optical pump-probe spectroscopy (OPPS), showing strong nonlinear layer-dependent responses.

4366–4373

Nano device

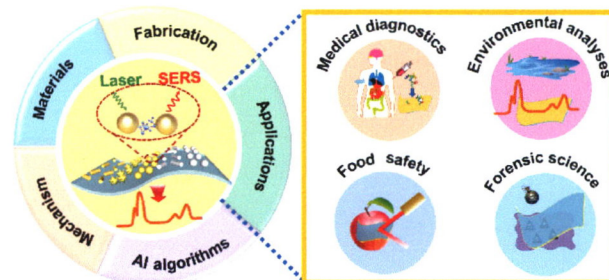
Review Article

State of the art in flexible SERS sensors toward label-free and onsite detection: From design to applications

Liping Xie^{1,*}, Hede Zeng¹, Jiaxin Zhu¹, Zelin Zhang¹, Hong-bin Sun¹, Wen Xia¹, and Yanan Du^{2,*}

¹ Northeastern University, China

² Tsinghua University, China



A state-of-the-art review of the flexible Surface-enhanced Raman scattering (SERS) sensors for point-of-care detection was provided from rational design to applications. Strategies of constructing the flexible SERS sensors were investigated in depth, enabling ultrasensitive detection of various analytes and high specificity with a fingerprint-like characteristic.

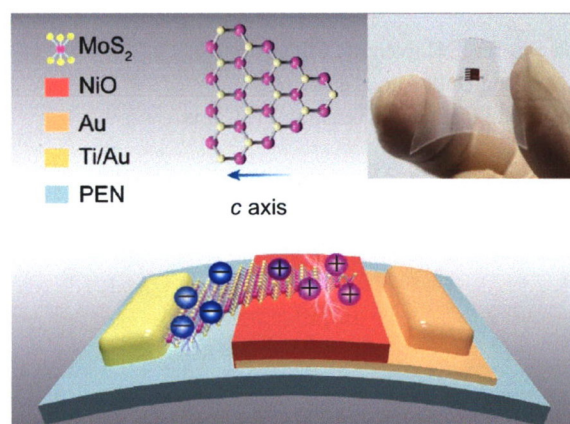
4374–4394

Research Articles

Fabry-Perot interference and piezo-phototronic effect enhanced flexible MoS₂ photodetector

Xuexia Chen, Xun Yang*, Qing Lou, Yuan Zhang, Yancheng Chen, Yacong Lu, Lin Dong*, and Chong-Xin Shan*

Zhengzhou University, China



Fabry-Perot (F-P) interference and piezo-phototronic effect are utilized to improve the performance of flexible MoS₂/NiO photodetectors (PDs). The flexible photodetector exhibits an ultrahigh detectivity (D^*) of 2.6×10^{14} Jones, which is the best value ever reported for flexible MoS₂ PDs.

4395–4402

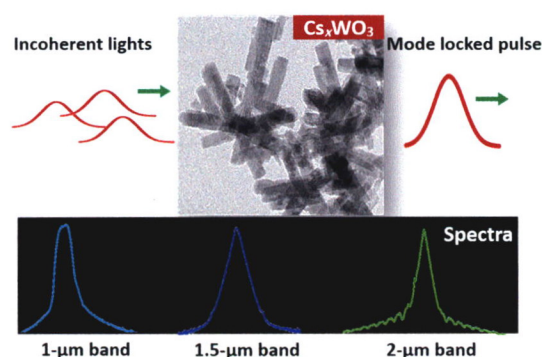
Nano-Cs₂WO₃: Ultra-broadband nonlinear optical modulator for near-infrared and mid-infrared ultrafast fiber lasers generation

Nan Li^{1,*}, Heng Jia², Ming Guo¹, Wenying Zhang¹, Ji Wang³, and Lijun Song^{1,*}

¹ Jilin Engineering Normal University, China

² Jilin University, China

³ Peng Cheng Laboratory, China



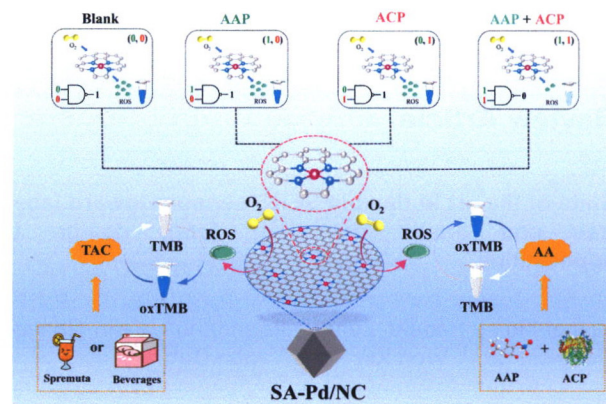
Cs₂WO₃ nanorods (NRs) as a novel ultra-broadband nonlinear optical modulator were successfully developed for ultrafast fiber lasers in three key wavelength bands from near-infrared (NIR) to mid-infrared (MIR) region.

4403–4410

Single-atom Pd catalysts as oxidase mimics with maximum atom utilization for colorimetric analysis

Zhe Li, Fangning Liu, Yuanyuan Jiang, Pengjuan Ni, Chenghui Zhang, Bo Wang, Chuanxia Chen*, and Yizhong Lu*

University of Jinan, China



Single-atom Pd catalysts as oxidase mimics with maximum atom utilization are successfully applied to assay the total antioxidant capacity of fruit, determine the serum acid phosphatase activity, and construct NAND logic gate.

4411–4420

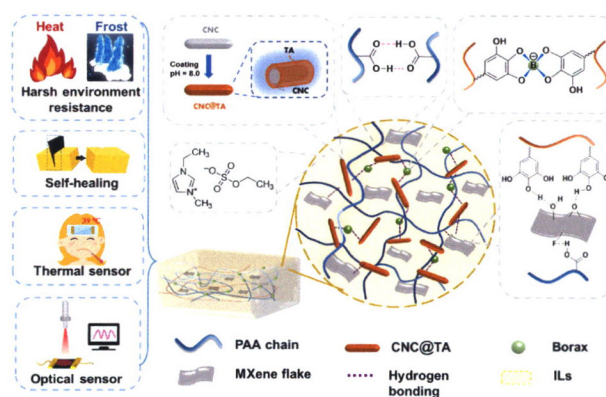
Ultradurable, freeze-resistant, and healable MXene-based ionic gels for multi-functional electronic skin

Yao Lu¹, Xinyu Qu¹, Siying Wang¹, Ye Zhao¹, Yanfang Ren², Wenli Zhao¹, Qian Wang^{1,*}, Chencheng Sun³, Wenjun Wang², and Xiaochen Dong^{1,*}

¹ Nanjing Tech University, China

² Liaocheng University, China

³ Changshu Institute of Technology, China



An ionic liquid incorporated and MXene-composited E-skin reveals highly durable and sensitive perception to multiple stimuli in harsh environments.

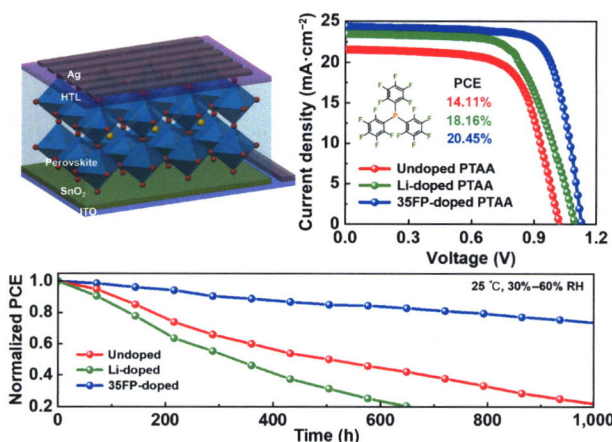
4421–4430

Stable and highly efficient perovskite solar cells: Doping hydrophobic fluoride into hole transport material PTAA

Chao Yu¹, Buyue Zhang^{1,2}, Chen Chen¹, Jintao Wang^{1,2}, Jian Zhang^{1,*}, Ping Chen¹, Chuannan Li¹, and Yu Duan^{1,*}

¹ Jilin University, China

² Changchun University of Science and Technology, China



The perovskite solar cells with 35FP-doped have better performance (PCE = 20.45%) compared with undoped device (PCE = 14.11%). The 35FP-doped devices only fell by 20% of its original efficiency after 1,000 h under ambient conditions without encapsulation.

4431–4438

Two-dimensional reconfigurable electronics enabled by asymmetric floating gate

Tengyu Jin^{1,2}, Jing Gao², Yanan Wang², Yue Zheng², Shuo Sun², Lei Liu³, Ming Lin⁴, and Wei Chen^{1,2,5,*}

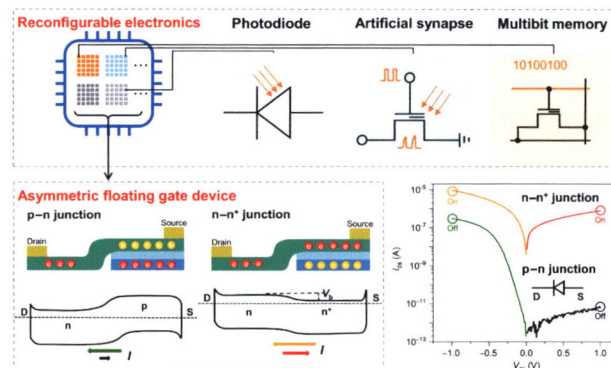
¹ International Campus of Tianjin University, China

² National University of Singapore, Singapore

³ Changchun Institute of Optics, Fine Mechanics and Physics, Chinese Academy of Sciences, China

⁴ Institute of Materials Research and Engineering (IMRE), Agency of Science, Technology, and Research (A*STAR), Singapore

⁵ National University of Singapore (Suzhou) Research Institute, China



A reconfigurable WSe₂ optoelectronic device is enabled by applying an asymmetric floating gate (AFG) into a flash memory, whose channel can be continuously programmed into p-n or n-n⁺ homojunctions by the AFG. As a result, a single AFG device can function as a photodiode, a 2-bit memory, or an artificial synapse under different working modes.

4439–4447

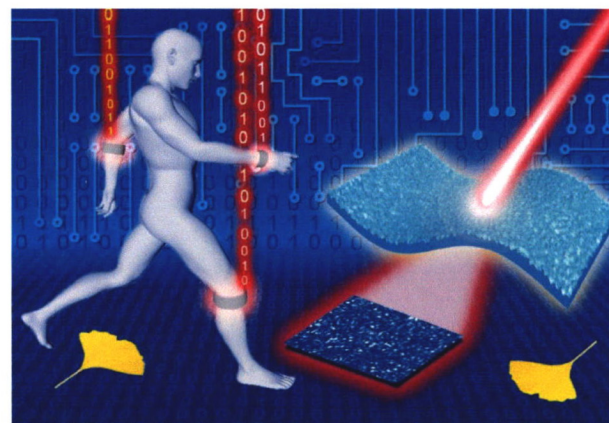
A flexible and stretchable bionic true random number generator

Yongbiao Wan^{1,2}, Kun Chen^{1,2}, Feng Huang^{1,2}, Pidong Wang^{1,2}, Xiao Leng^{1,2}, Dong Li^{1,2}, Jianbin Kang^{1,2}, Zhiguang Qiu^{3,*}, and Yao Yao^{1,2,*}

¹ Microsystem and Terahertz Research Center, China Academy of Engineering Physics, China

² Institute of Electronic Engineering, China Academy of Engineering Physics, China

³ Sun Yat-sen University, China



A flexible and stretchable bionic true random number generator (TRNG) is inspired by biological uniqueness and randomness. Random numbers extracted from laser speckle patterns of the flexible TRNG show superior randomness, robustness, and potential in application of flexible networked electronics.

4448–4456

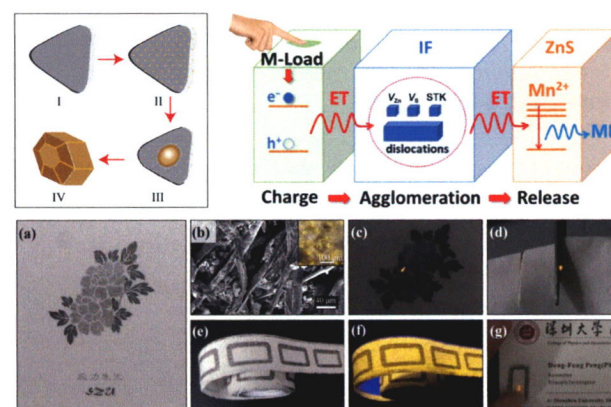
Interface synergistic effects induced multi-mode luminescence

Ronghua Ma¹, Chunfeng Wang¹, Wei Yan¹, Mingzi Sun², Jianxiong Zhao³, Yuntian Zheng¹, Xu Li¹, Longbiao Huang¹, Bing Chen³, Feng Wang³, Bolong Huang^{2,*}, and Dengfeng Peng^{1,*}

¹ Shenzhen University, China

² The Hong Kong Polytechnic University, China

³ City University of Hong Kong, Hong Kong, China



Mechanoluminescence has attracted intensive intentions due to their flexible properties and robust performances for broad applications. However, the development is usually limited in the single-phase materials. We synthesize the heterostructure biphas ZnS:Mn, which delivers efficient mechanoluminescence (ML) due to the abundant defects at the interfaces. The successful applications of ZnS:Mn in ink and papers open its potential in the future.

4457–4465

Nano unit

Highlight

Tempering force with mercy: An innovative peri-implant ligament with combined osteointegration and energy-dissipation

Xun Wang*

Tsinghua University, China

4466–4467

Review Article

Past, present and future of indium phosphide quantum dots

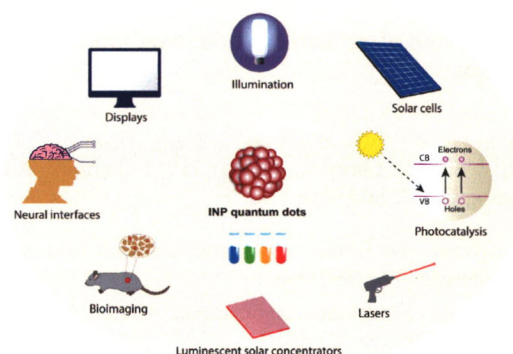
Houman Bahmani Jalali^{1,†}, Sadra Sadeghi^{2,‡}, Itir Bakis Dogru Yukse^{2,⊥}, Asim Onal³, and Sedat Nizamoglu^{1,2,3,*}

Koç University, Turkey

[†] Present address: Istituto Italiano di Tecnologia, Italy

[‡] Present address: Queen's University, Canada

[⊥] Present address: Utrecht University, the Netherlands



This review focuses on the history, recent development, and future aspect of synthesis and application of colloidal indium phosphide (InP) quantum dots (QDs).

4468–4489

Research Articles

Phase constitution of the noble metal thin-film complex solid solution system Ag-Ir-Pd-Pt-Ru in dependence of elemental compositions and annealing temperatures

Tingting Zou^{1,2}, Bo Zhao⁴, Wei Xin^{1,3,*}, Feiyue Wang^{1,2}, Hongbo Xie^{1,2}, Yuhang Li^{1,2}, Yuwei Shan¹, Kun Li⁵, Yanbing Sun⁵, and Jianjun Yang^{1,*}

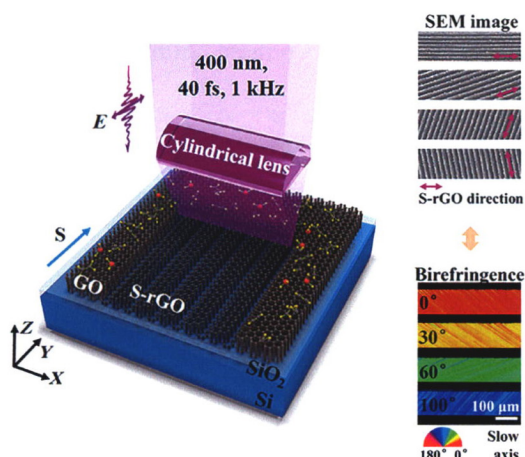
¹ Changchun Institute of Optics, Fine Mechanics and Physics, Chinese Academy of Sciences, China

² University of Chinese Academy of Sciences, China

³ Northeast Normal University, China

⁴ Changzhi University, China

⁵ Changchun New Industries Optoelectronics Technology Co., Ltd, China



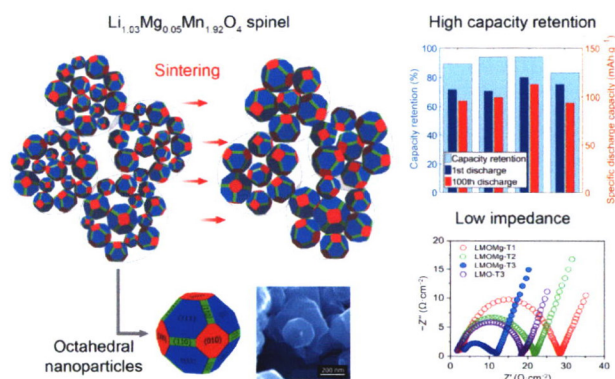
This article develops a feasible scheme for the high-speed preparation of large-area in-plane anisotropic photoelectronic graphene oxide thin film (< 100 nm), which is compatible with existing semi-conductor manipulation processes. This will also promote the preparation of industrial integrated devices.

4490–4499

Potential use of magnesium industrial waste for synthesis of Li and Mg co-doped LiMn_2O_4 nanoparticles as cathode material for Li-ion batteries: Effect of sintering temperature

Aleksei Llusco, Luis Rojas, Svetlana Ushak, and Mario Grageda*

Universidad de Antofagasta, Chile



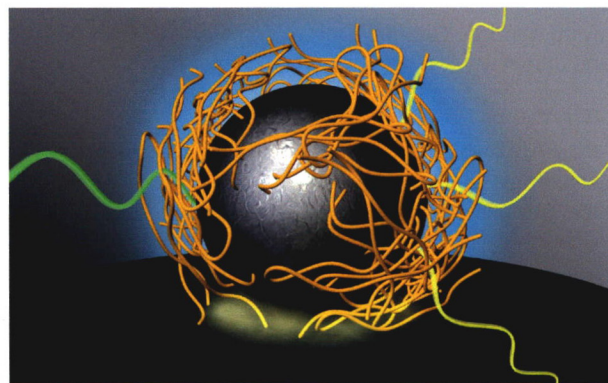
The use of $\text{Mg}(\text{OH})_2$ for synthesis of Li and Mg co-doped LiMn_2O_4 (LMO) spinel nanoparticles at a sintering temperature of 750 °C is a potential strategy for development of cathode materials with high-rate capability and long cycling stability for lithium-ion (Li-ion) batteries, as well as for recovery of valuable resources from industrial waste generated in the production of Li_2CO_3 .

4500–4516

Operando electrochemical SERS monitors nanoparticle reactions by capping agent fingerprints

Kevin Wonner, Steffen Murke, Serena R. Alfaraño, Pouya Hosseini, Martina Havenith*, and Kristina Tschulik

Ruhr University Bochum, Germany



Capping agent effects on the electrochemical oxidation of silver nanoparticles (NPs) are studied in halide electrolyte solutions by coupled electrochemical surface-enhanced Raman spectroscopy (SERS). The reaction is directly monitored by the current response and the simultaneous Raman signal.

4517–4524

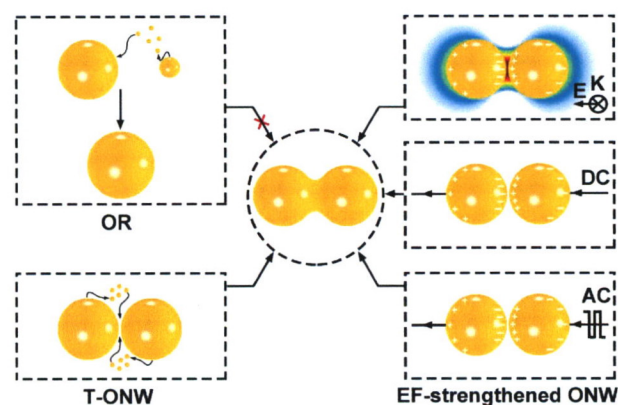
External field-strengthened Ostwald nanowelding

Moxia Li¹, Xi Xie², Yaomengli Xu¹, Jianfang Liu¹, Yanan Fu², Mei Han¹, Xucheng Li³, Xidong Duan^{1,*}, Changjun Min^{2,*}, and Jiawen Hu^{1,*}

¹ Hunan University, China

² Shenzhen University, China

³ Xiamen University, China



The accomplishment of nanowelding typically requires the input of high energy, possibly causing appreciable damages to the brittle nanomaterial. This study reports an external field (EF, i.e., light, direct current (DC), and alternating current (AC))-strengthened Ostwald nanowelding (ONW) strategy to enable low-temperature nanowelding of Au nanoparticles (NPs) with nanoscale spacing in solution and proposes an electron localization mechanism to understand it.

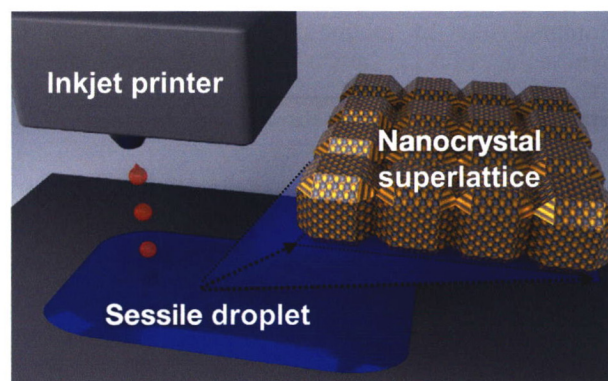
4525–4535

Inkjet printing of epitaxially connected nanocrystal superlattices

Daniel M. Balazs[†], N. Deniz Erkan, Michelle Quien, and Tobias Hanrath^{*}

Cornell University, USA

[†] Present address: Institute of Science and Technology Austria, Austria



Monolayer TiSe_2 with Pt adatoms adsorption on the line defects was successfully fabricated on the $\text{Au}(111)$ substrate. The density functional theory calculations show that the line defect itself has catalytic activity for hydrogen evolution reaction, and it will have better catalytic activity if it adsorbs Pt atoms.

4536–4543

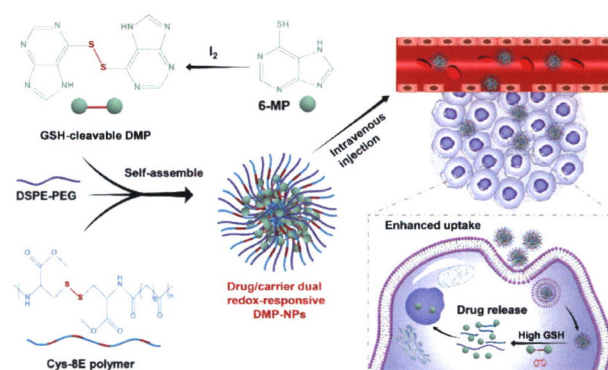
A drug/carrier dual redox-responsive system based on 6-mercaptopurine dimer-loaded cysteine polymer nanoparticles for enhanced lymphoma therapy

Liyang Wang¹, Chunlei Dai¹, Yifen Fang², Xinru You^{1,3,*}, and Jun Wu^{1,*}

¹ Sun Yat-sen University, China

² the Affiliated TCM Hospital of Guangzhou Medical University, China

³ the Seventh Affiliated Hospital of Sun Yat-sen University, China



Traditional anticancer drug 6-mercaptopurine was dimerized and then encapsulated by a cysteine-based polymer to form a drug/carrier dual redox-responsive nanoplateform (DMP-NPs). The DMP-NPs achieved controllable drug release, enhanced tumor accumulation, and improved the anticancer effect against lymphoma therapy with high safety.

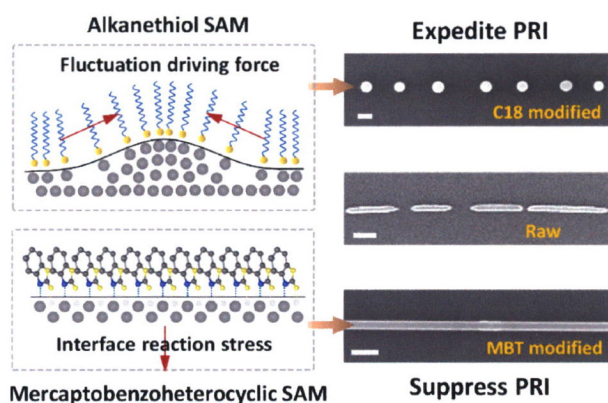
4544–4551

Self-assembled monolayer modulated Plateau-Rayleigh instability and enhanced chemical stability of silver nanowire for invisibly patterned, stable transparent electrodes

Gui-Shi Liu¹, Huajian Zheng¹, Zijie Zeng¹, Yexiong Wang¹, Weidong Guo¹, Ting Wang³, Heng Chen¹, Yunsen Chen¹, Shiqi Hu¹, Lei Chen¹, Yaofei Chen¹, Weiguang Xie¹, Bo-Ru Yang^{2,*}, and Yunhan Luo^{1,*}

¹ Jinan University, China

² Sun Yat-sen University, China



The control on Plateau-Rayleigh instability (PRI) of silver nanowire (AgNW) is readily realized by two kinds of self-assembled monolayers (SAMs), which not only provides the AgNW with superior anti-corrosion but also enables achieving invisible patterning of the AgNW network.

4552–4562

Coupled Tamm plasmon polaritons induced narrow bandpass filter with ultra-wide stopband

Qingquan Liu^{1,2,3,4}, Xinchao Zhao^{1,3,4}, Chenlu Li^{1,2,3,4}, Xinglei Zhou^{1,4}, Yu Chen¹, Shaowei Wang^{1,3,4,5,*}, and Wei Lu^{1,2,3,4,5,*}

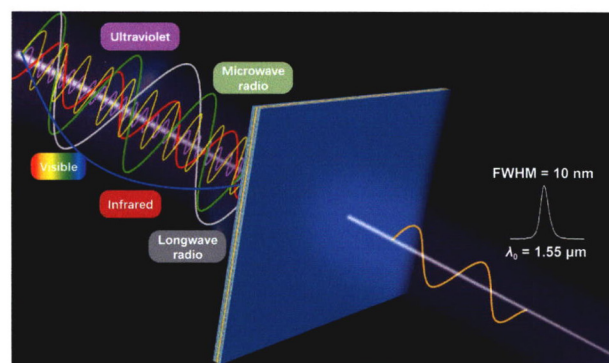
¹ Shanghai Institute of Technical Physics, Chinese Academy of Sciences, China

² ShanghaiTech University, China

³ University of Chinese Academy of Sciences, China

⁴ Shanghai Engineering Research Center of Energy-Saving Coatings, China

⁵ Shanghai Research Center for Quantum Sciences, China



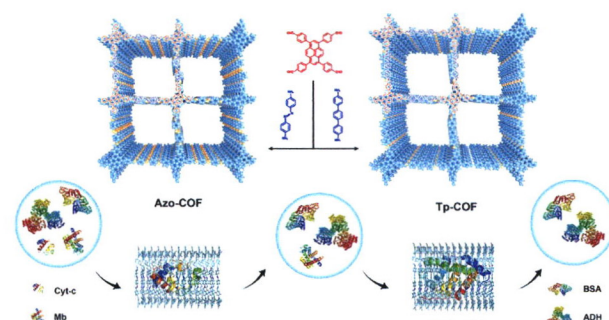
A narrow bandpass filter (NBPF) with ultra-wide stopband based on the coupled Tamm plasmon polaritons (TPPs) transmission theory is proposed and fabricated. It only allows the light with a wavelength of 1.55 μm to pass through and shields light with other wavelengths. This performance is much better than the traditional filters and those reported novel metamaterial filters.

4563–4568

Fine-tuned mesoporous covalent organic frameworks for highly efficient low molecular-weight proteins separation

Tienan Wang, Irfan Azhar, Yuting Yang, Yao Lu, Yuyang Tian, Nan Gao, Fengchao Cui*, Li Yang*, Xiaofei Jing*, and Guangshan Zhu

Northeast Normal University, China



Two stable mesoporous covalent organic frameworks with well-regulated channels were synthesized and exhibited highly efficient size-selective separation for low molecular-weight proteins.

4569–4574

Bending strain effects on the optical and optoelectronic properties of GaN nanowires

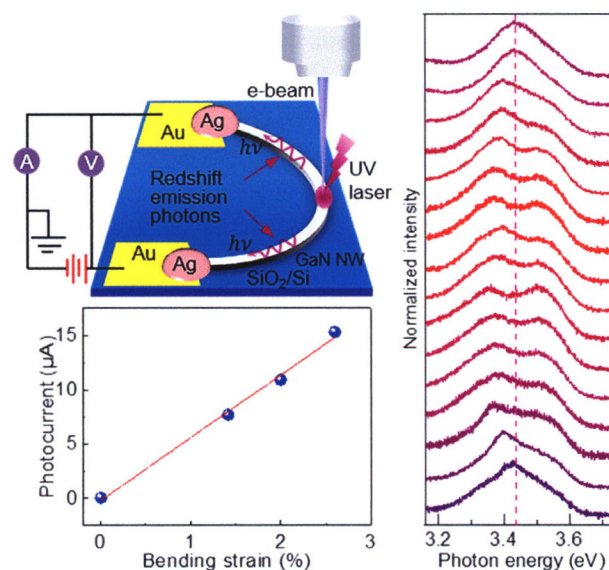
Xuewen Fu^{1,*}, Haixia Nie¹, Zepeng Sun¹, Min Feng¹, Xiang Chen¹, Can Liu¹, Fang Liu¹, Dapeng Yu², and Zhimin Liao^{3,4,*}

¹ Nankai University, China

² Southern University of Science and Technology, China

³ Peking University, China

⁴ Peking University Yangtze Delta Institute of Optoelectronics, China



Elastic bending strain induces extraordinary splitting of near band emission and compelling enhancement of ultraviolet photoresponse in GaN nanowires.

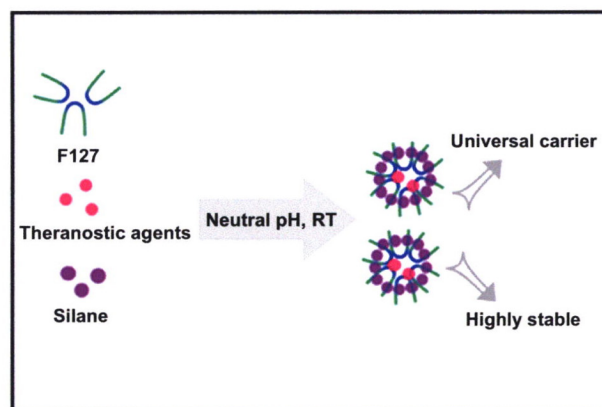
4575–4581

Highly stable hybrid single-micelle: A universal nanocarrier for hydrophobic bioimaging agents

Qiaoyu Zhou¹, Tiancong Zhao¹, Mengli Liu¹, Dongrui Yin¹, Minchao Liu¹, Ahmed A. Elzatahry², Fan Zhang¹, Dongyuan Zhao¹, and Xiaomin Li^{1,*}

¹ Fudan University, China

² Qatar University, Qatar



Highly stable hybrid single-micelles (ICG@H-micelles) are synthesized under mild conditions and exhibit improved structural and fluorescence stability.

4582–4589

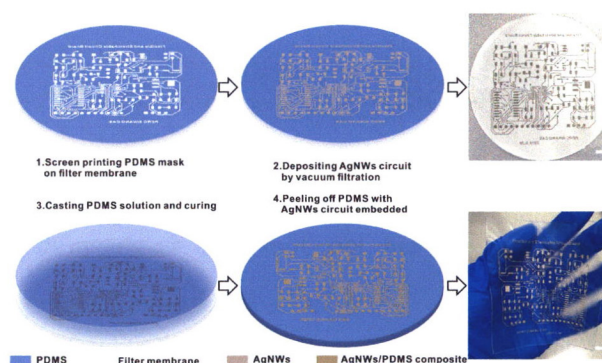
High-resolution and large-size stretchable electrodes based on patterned silver nanowires composites

Yong Lin¹, Qingsong Li², Chen Ding¹, Jiayi Wang^{1,3}, Wei Yuan^{1,*}, Zhiyuan Liu², Wenming Su¹, and Zheng Cui^{1,*}

¹ Suzhou Institute of Nano-Tech and Nano-Bionics, Chinese Academy of Sciences, China

² Shenzhen Institute of Advanced Technology, Chinese Academy of Sciences, China

³ University of Science and Technology of China, China



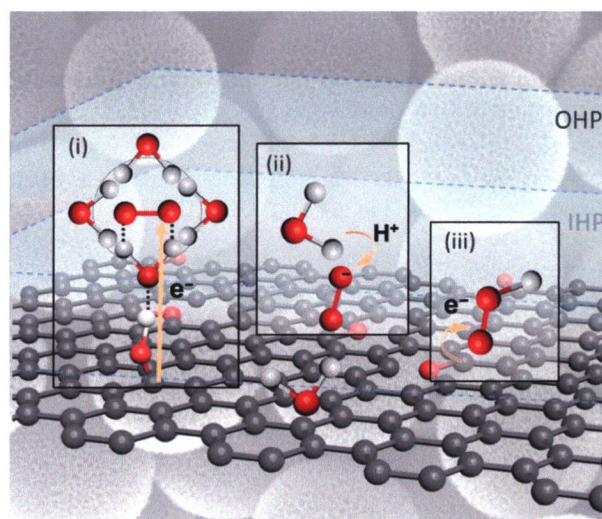
A method was developed for preparing high-resolution, large-size stretchable electrodes by pre-constructing silver nanowires (AgNWs) patterns through screen printing and vacuum filtration then embedding them into a polydimethylsiloxane (PDMS) matrix. These electrodes have been successfully used as a large-size stretchable circuit board for a smart display system and an 18-channel high-density electrode array for surface electromyography (EMG) recording.

4590–4598

Mechanism investigation of enhanced electrochemical H₂O₂ production performance on oxygen-rich hollow porous carbon spheres

Zhiping Deng and Xiaolei Wang*

University of Alberta, Canada



Oxygen functionalization on the hollow mesoporous carbon spheres (HMCSSs) results in improved reactivity of these active sites, hydrophilic property of the surface, and tuned adsorption mode of oxygen, leading to significantly reduced overpotential, improved selectivity, and moderate stability for oxygen reduction to H₂O₂.

4599–4605

Dehydro-Diels–Alder reaction and diamondization of bowl-shaped clusters $C_{18}Te_3Br_4(Bu-O)_6$

Jinbo Zhang^{1,2}, Manli Ma¹, Rong Zhou¹, Hongqiang Chu¹, Xue Wang¹, Shaojie Wang², Huhu Tian^{3,4}, Zhipeng Yan⁵, Mingtao Li⁶, Zhongyan Wu⁷, Bin Li⁷, Jiafeng Yan⁷, Lan Anh Thi Nguyen⁷, Rongxing Cao¹, Guoqing Wu¹, Xianghua Zeng¹, Hao-Li Zhang^{3,*}, Jaeyong Kim^{7,*}, Lin Wang^{2,*}, and Yongjun Tian²

¹ Yangzhou University, China

² Yanshan University, China

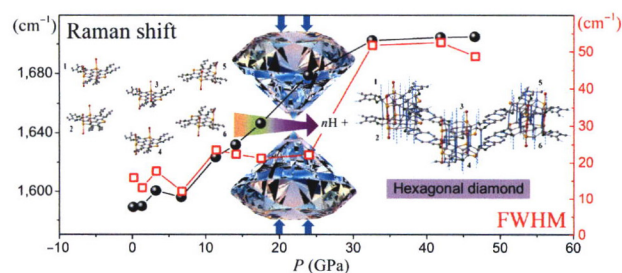
³ Lanzhou University, China

⁴ Baotou Research Institute of Rare Earths, China

⁵ Southern University of Science and Technology, China

⁶ Center for High Pressure Science and Technology Advanced Research, China

⁷ Hanyang University, Republic of Korea



Pressure-induced dehydro-Diels–Alder reaction occurred at ~ 7 GPa. Above 17.0 GPa, the intermolecular sp^3 bonding was built up in an amorphous state, that is pressure-induced diamondization. Dehydro-Diels–Alder reaction (decomposition) and diamondization (polymerization) specify the solid-state topochemical reaction, those are scarcely seen in solid-state. The pressure dependence of G band in Raman spectroscopy reflected $C_{18}Te_3Br_4(Bu-O)_6$ evolution with pressure.

4606–4612

Semiconductor

Review Article

Emerging Internet of Things driven carbon nanotubes-based devices

Shu Zhang¹, Jinbo Pang^{1,*}, Yufen Li¹, Feng Yang^{2,*}, Thomas Gemming³, Kai Wang⁵, Xiao Wang⁶, Songang Peng⁷, Xiaoyan Liu¹, Bin Chang¹, Hong Liu^{1,4,*}, Weijia Zhou¹, Gianaurelio Cuniberti^{11,*}, and Mark H. Rummeli^{3,8,9,10}

¹ University of Jinan, China

² Southern University of Science and Technology, China

³ Leibniz Institute for Solid State and Materials Research Dresden, Germany

⁴ Shandong University, China

⁵ Qingdao University China

⁶ Shenzhen Institutes of Advanced Technology, Chinese Academy of Sciences, China

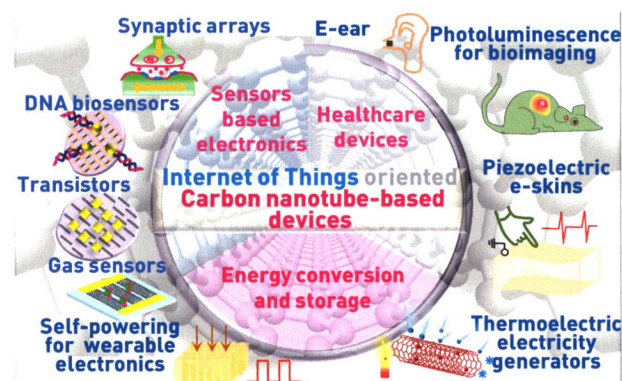
⁷ Institute of Microelectronics, Chinese Academy of Sciences, China

⁸ Soochow University, China

⁹ Centre of Polymer and Carbon Materials, Polish Academy of Sciences, Poland

¹⁰ VŠB-Technical University of Ostrava, Czech Republic

¹¹ Technische Universität Dresden, Germany



This review provides the most advances of electronic devices applications of carbon nanotubes driven by the Internet of Things (IoT), including the transistor arrays, sensors, healthcare systems, and energy devices.

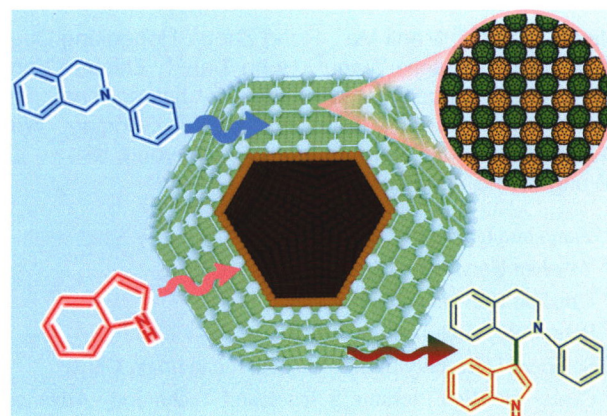
4613–4637

Research Articles

Fabricating a hollow cuboctahedral structure for N-doped carbon coated p-n heterojunctions towards high-performance photocatalytic organic transformation

Hao Gao, Liming Sun, Mengge Li, Wenwen Zhan*, Xiaojun Wang, and Xiguang Han

Jiangsu Normal University, China



A novel hollow cuboctahedral nanostructure composed of N-doped carbon layer and CuO/NiO heterojunctions has been successfully fabricated as the photocatalyst of cross-dehydrogenative coupling (CDC) reactions.

4638–4645

Selective hydrogenation improves interface properties of high-*k* dielectrics on 2D semiconductors

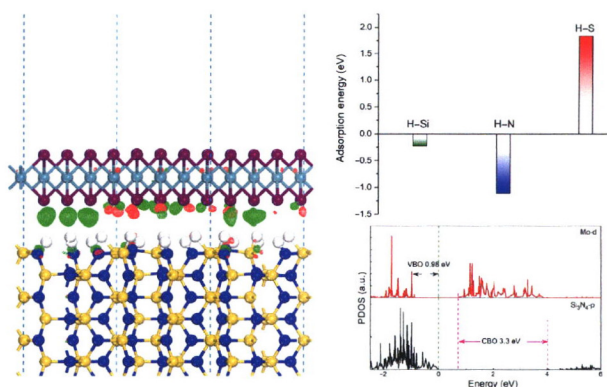
Yulin Yang¹, Tong Yang², Tingting Song³, Jun Zhou⁴, Jianwei Chai⁴, Lai Mun Wong⁴, Hongyi Zhang¹, Wenzhang Zhu¹, Shijie Wang^{4,*}, and Ming Yang^{2,*}

¹ Xiamen University of Technology, China

² The Hong Kong Polytechnic University, Hong Kong, China

³ China West Normal University, China

⁴ Institute of Materials Research and Engineering, Agency for Science, Technology and Research (A*STAR), Singapore



The hydrogenation process can passivate the interface states at the high-*k* dielectrics, but does not affect the two-dimensional (2D) semiconductors, enabling an improved integration of high-*k* dielectrics on 2D materials based nanoelectronics.

4646–4652

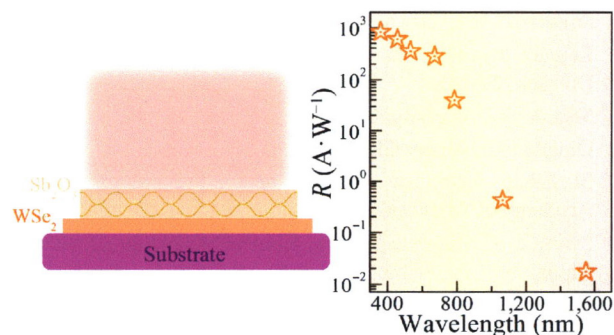
Broadband light absorption and photoresponse enhancement in monolayer WSe₂ crystal coupled to Sb₂O₃ microresonators

Kun Ye¹, Lixuan Liu^{1,2}, Congpu Mu^{1,*}, Kun Zhai^{1,*}, Shiliang Guo¹, Bochong Wang¹, Anmin Nie¹, Shuhan Meng¹, Fusheng Wen¹, Jianyong Xiang¹, Tianyu Xue¹, Ming Kang³, Yongji Gong², Yongjun Tian¹, and Zhongyuan Liu^{1,*}

¹ Yanshan University, China

² Beihang University, China

³ Tianjin Normal University, China



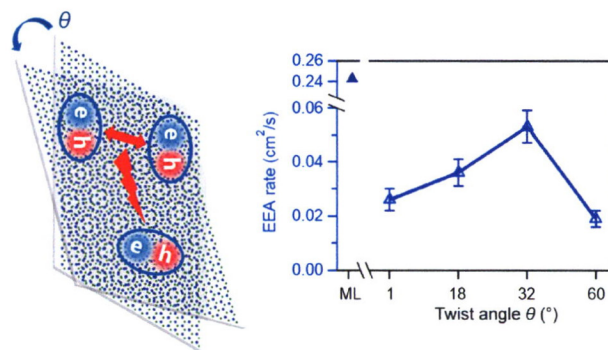
The significantly enhanced visible and expanded near infrared (NIR) light absorption of monolayer WSe₂ on integration with triangular Sb₂O₃ microresonators in wide thickness and lateral size distributions. As a photodetector, monolayer transition metal dichalcogenides (TMDCs) crystal coupled to Sb₂O₃ microresonators has been observed to exhibit the enhanced responsivity by at least or nearly 10⁴ order in visible light region and the expanded one of ~ 1 A·W⁻¹ in NIR range, better than most of the reported photodetectors based on monolayer TMDCs.

4653–4660

Controlling exciton-exciton annihilation in WSe₂ bilayers via interlayer twist

Yuzhong Chen, Bichuan Cao, Cheng Sun, Zedong Wang, Hongzhi Zhou, Linjun Wang*, and Haiming Zhu*

Zhejiang University, China



By combining ultrafast spectroscopy and first-principles calculation, we show that the twist angle in transition metal dichalcogenide (TMD) bilayers can act as an effective knob to tune the exciton-exciton annihilation dynamics.

4661–4667

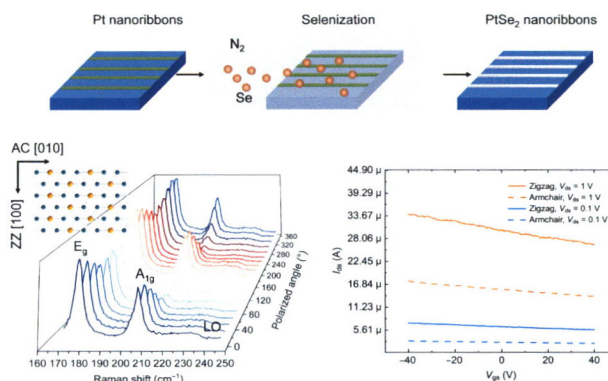
Anisotropic electrical properties of aligned PtSe₂ nanoribbon arrays grown by a pre-patterned selective selenization process

Huaipeng Wang¹, Zhifang Liu¹, Yilin Sun^{2,*}, Xiaofan Ping¹, Jianlong Xu³, Yingtao Ding², Haowen Hu¹, Dan Xie^{1,*}, and Tianling Ren^{1,*}

¹ Tsinghua University, China

² Beijing Institute of Technology, China

³ Soochow University, China



Anisotropic electrical properties of naturally aligned zigzag PtSe₂ nanoribbon arrays were investigated through angle-resolved polarized Raman spectroscopy and electrical measurements. The underlying mechanism of its selective growth and anisotropic conductivities are revealed using density functional theory and semi-classic Boltzmann transport theory.

4668–4676

Synthesis

Research Articles

Ultrafast growth of high-quality large-sized GaSe crystals by liquid metal promoter

Zuxin Chen^{1,5,6}, Quan Chen¹, Zebing Chai¹, Bin Wei², Jun Wang³, Yanping Liu⁴, Yumeng Shi^{5,*}, Zhongchang Wang^{6,*}, and Jingbo Li^{1,*}

¹ South China Normal University, China

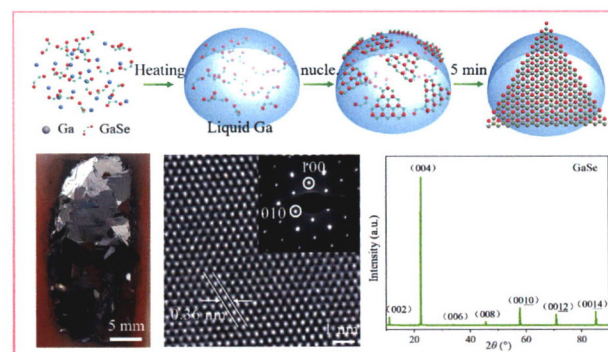
² Sun Yat-Sen University, China

³ Wuhan University, China

⁴ Central South University, China

⁵ Shenzhen University, China

⁶ International Iberian Nanotechnology Laboratory, Portugal



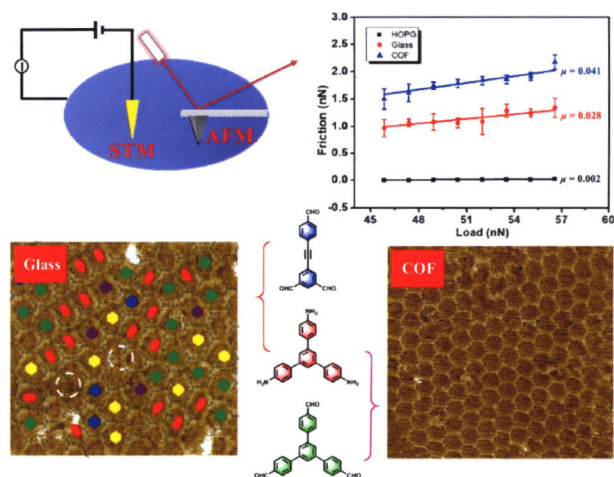
A liquid-metal-assisted chemical vapor deposition method is proposed to rapidly synthesize centimeter-sized GaSe crystals of high crystal quality, which show good performance of photodetector.

4677–4681

Construction and nanotribological study of a glassy covalent organic network on surface

Guangyuan Feng, Qingqing Luo, Mengqi Li, Yaru Song, Yongtao Shen*, Shengbin Lei*, and Wenping Hu*

Tianjin University, China



The large-scale, continuous, and low-defect glassy covalent organic networks (GCONs) was constructed based on dynamic covalent chemistry on surface, and the GCONs have lower friction coefficient in comparison with crystalline covalent organic frameworks (COFs).

4682–4686

Line defects in monolayer TiSe_2 with adsorption of Pt atoms potentially enable excellent catalytic activity

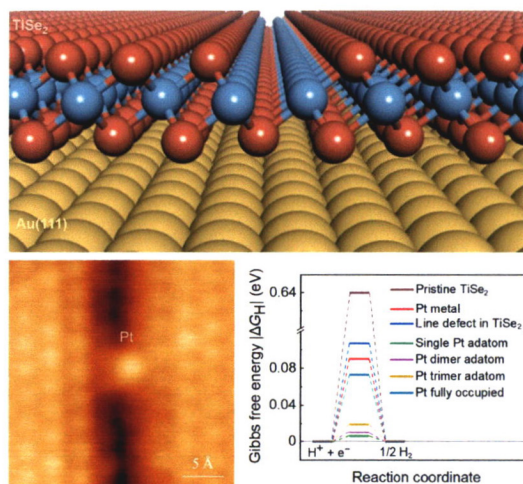
Zhipeng Song¹, Juxia Yi¹, Jing Qi¹, Qi Zheng¹, Zhili Zhu¹, Lei Tao¹, Yun Cao¹, Yan Li¹, Zhaoyan Gao¹, Ruizi Zhang^{1,*}, Li Huang¹, Geng Li^{1,2,3}, Ziqiang Xu⁴, Xu Wu⁴, Yeliang Wang⁴, Chengmin Shen^{1,2}, Yu-Yang Zhang^{1,2}, Hongliang Lu^{1,2,*}, Xiao Lin^{1,2,*}, Shixuan Du^{1,2,3}, and Hong-Jun Gao^{1,2,3}

¹ Institute of Physics and University of Chinese Academy of Sciences, Chinese Academy of Sciences, China

² CAS Center for Excellence in Topological Quantum Computation, Chinese Academy of Sciences, China

³ Songshan Lake Materials Laboratory, China

⁴ Beijing Institute of Technology, China



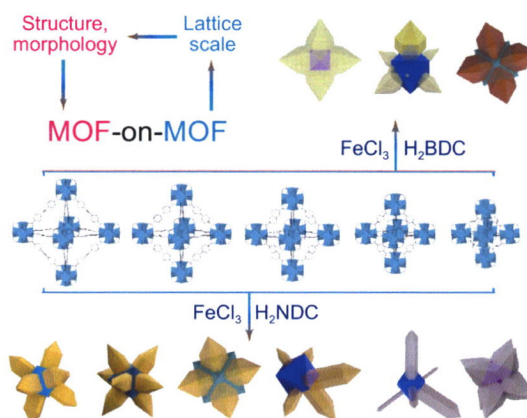
Monolayer TiSe_2 with Pt adatoms adsorption on the line defects were successfully fabricated on the Au(111) substrate. The density functional theory calculations shows that the line defect itself has catalytic activity for hydrogen evolution reaction, and it will have better catalytic activity if it adsorbs Pt atoms.

4687–4692

Flexible-on-rigid heteroepitaxial metal-organic frameworks induced by template lattice change

XiaoGang Wang, Han Cheng*, and XianZheng Zhang*

Wuhan University, China



The modulation of chemical composition and framework topology on the molecular scale, and adjustment of morphology on the mesoscale were achieved during the construction of flexible-on-rigid hybrid-phase metal-organic frameworks.

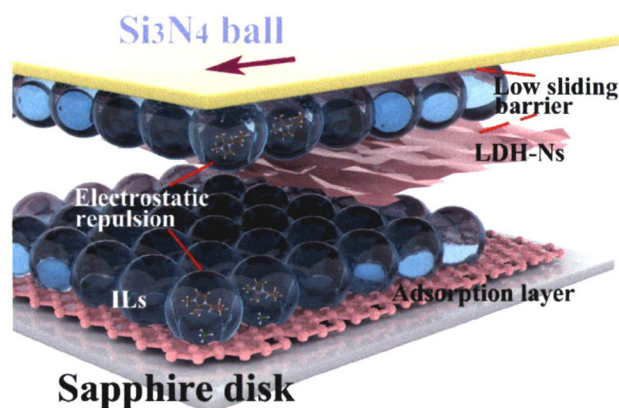
4693–4699

Macroscale superlubricity under ultrahigh contact pressure in the presence of layered double hydroxide nanosheets

Kunpeng Wang¹, Lei Liu¹, Aisheng Song¹, Tianbao Ma¹, Hongdong Wang^{1,2,*}, Jianbin Luo^{1,*}, and Yuhong Liu^{1,*}

¹ Tsinghua University, China

² Shanghai University, China



Macroscale superlubricity under ultrahigh contact pressure was enabled by the combination of layered double hydroxide nanosheets with ionic liquid.

4700–4709

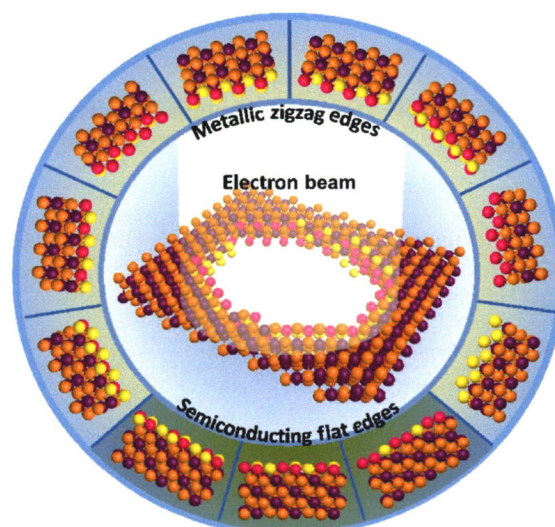
Tailoring Bi₂Te₃ edge with semiconductor and metal properties under electron beam irradiation

Yuting Shen^{1,2}, Hailin Yu^{1,*}, Tao Xu², Qiubo Zhang^{2,3}, Kuibo Yin², Shan Cong¹, Yushen Liu¹, and Litao Sun^{2,*}

¹ Changshu Institute of Technology, China

² Southeast University, China

³ Lawrence Berkeley National Laboratory, USA



Electron beam irradiation can be utilized to tailor single-layer Bi₂Te₃ with semiconducting flat edges and metallic zigzag edges with atomic resolution.

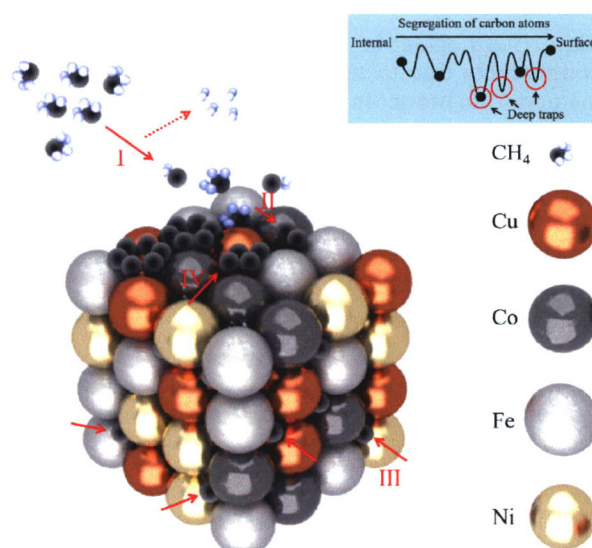
4710–4716

Intrinsic-trap-regulating growth of clean graphene on high-entropy alloy substrate

Ning Cao¹, Peng Liu¹, Jialiang Pan², Liheng Liang¹, Kunpeng Cai¹, Qingguo Shao¹, Hongwei Zhu^{2,*}, and Xiaobei Zang^{1,*}

¹ China University of Petroleum (East China), China

² Tsinghua University, China



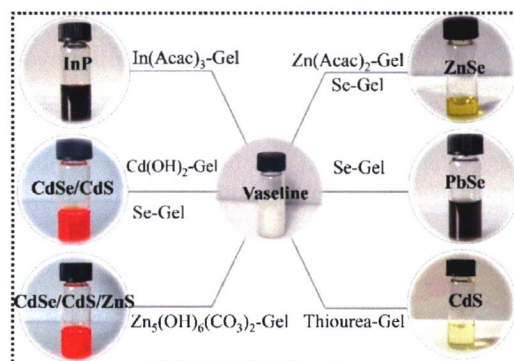
A facile approach to grow few-layer graphene on high-entropy alloy (FeCoNiCu₂) is presented and the growth mechanism of graphene is systematically investigated.

4717–4723

Universal precursors dispersed in Vaseline-octadecene gel for nanocrystal synthesis

Xiaofei Hu, Jiongzhao Li*, Zhe Wang, Xudong Qian, Chenqi Zhu, and Xiaogang Peng*

Zhejiang University, China



Small molecules in hydrocarbon gels are ideal precursors for synthesizing inorganic nanocrystals.

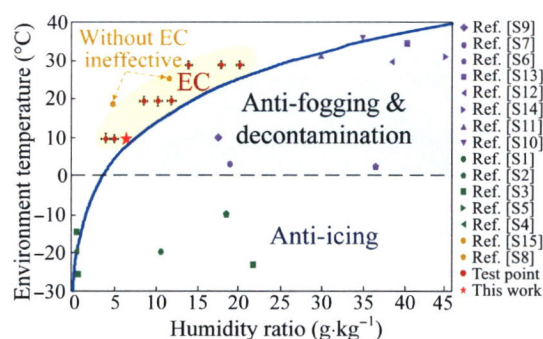
4724–4731

Self-cleaning of superhydrophobic nanostructured surfaces at low humidity enhanced by vertical electric field

Yijie Liu¹, Yujun Guo^{1,*}, Xueqin Zhang¹, Guoqiang Gao¹, Chaoqun Shi¹, Guizao Huang¹, Pengli Li², Qi Kang², Xingyi Huang^{2,*}, and Guangning Wu^{1,*}

¹ Southwest Jiaotong University, China

² Shanghai Jiaotong University, China



This paper realized the self-cleaning of superhydrophobic nanostructured surfaces above the dew point curve for the first time with the assistance of an electric field.

4732–4738

High thermoelectric properties with low thermal conductivity due to the porous structure induced by the dendritic branching in n-type PbS

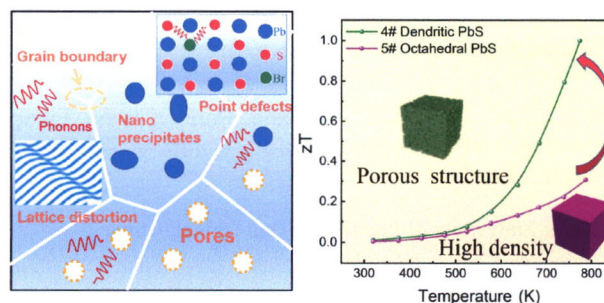
Zhenyu Zhu¹, Janak Tiwari², Tianli Feng², Zhan Shi³, Yue Lou^{1,*}, and Biao Xu^{1,4,*}

¹ Nanjing University of Science and Technology, China

² The University of Utah, USA

³ Jilin University, China

⁴ Nanjing University, China



The difference in morphology of PbS nanocrystals leads to different stackings, tunable thermal conductivity. Ultimately the zT value of the porous structure (4#) is greatly improved under the multiple phonons scattering mechanism as compared to the high-density sample (5#).

4739–4746

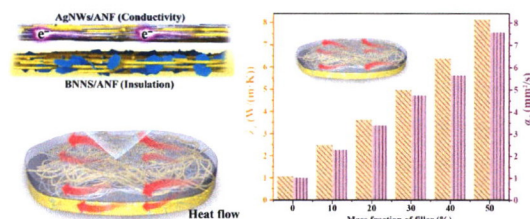
Janus (BNNS/ANF)-(AgNWs/ANF) thermal conductivity composite films with superior electromagnetic interference shielding and Joule heating performances

Yixin Han^{1,2}, Kunpeng Ruan^{1,2}, and Junwei Gu^{1,2,*}

¹ Research & Development Institute of Northwestern Polytechnical University in Shenzhen, China

² Northwestern Polytechnical University, China

4747–4755



Janus (BNNS/ANF)-(AgNWs/ANF) thermal conductivity and electromagnetic interference shielding composite films exhibit “one side insulating, one side conducting” performance. And Janus (BNNS/ANF)-(AgNWs/ANF) composite film with thickness of 95 μm has a high in-plane thermal conductivity coefficient of 8.12 W/(m·K) and superior electromagnetic interference shielding effectiveness of 70 dB.

Smart ZnS@C filler for super-anticorrosive self-healing zinc-rich epoxy coating

Kai Yang^{1,2}, Yixue Duan³, Guicheng Liu^{2,*}, Guoyan Ma⁴, Hao Fu², Xuyong Chen¹, Manxiang Wang², Gangqiang Zhu⁵, Wochul Yang^{2,*}, and Yiding Shen^{1,*}

¹ Shaanxi University of Science and Technology, China

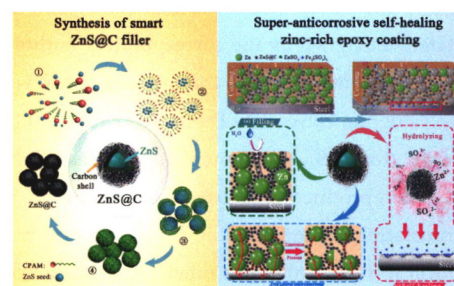
² Dongguk University, Republic of Korea

³ Wuhan University of Technology, China

⁴ Xi'an Shiyou University, China

⁵ Shaanxi Normal University, China

4756–4764



Uniform carbon-coated ZnS (ZnS@C) nanoballs, as smart fillers, were synthesized to design super-anticorrosive self-healing zinc-rich epoxy coatings for protecting marine steel. The nano-size, C-shell, and ZnS-core of the smart filler enhance pore filling efficiency, active Zn-site amount, and self-healing effect, respectively, leading to efficient shielding protection and extended cathodic protection time.

Theory

Research Article

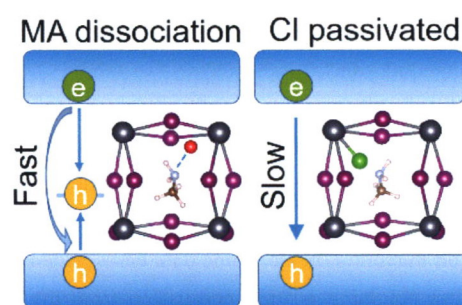
Chemical passivation of methylammonium fragments eliminates traps, extends charge lifetimes, and restores structural stability of $\text{CH}_3\text{NH}_3\text{PbI}_3$ perovskite

Xi Zhao¹, Wei-Hai Fang¹, Run Long^{1,*}, and Oleg V. Prezhdo²

¹ Beijing Normal University, China

² University of Southern California, Los Angeles, USA

4765–4772



Dissociation of the methylammonium cation in $\text{CH}_3\text{NH}_3\text{PbI}_3$ undermines structural stability, produces deep hole traps, and decreases charge carrier lifetimes. Passivating methylammonium fragments with chlorines restores the stability, eliminates the traps, and makes charge lifetimes even longer than in pristine $\text{CH}_3\text{NH}_3\text{PbI}_3$.

Erratum to: Different micro/nano-scale patterns of surface materials influence osteoclastogenesis and actin structure (<https://doi.org/10.1007/s12274-021-4026-3>)

4773

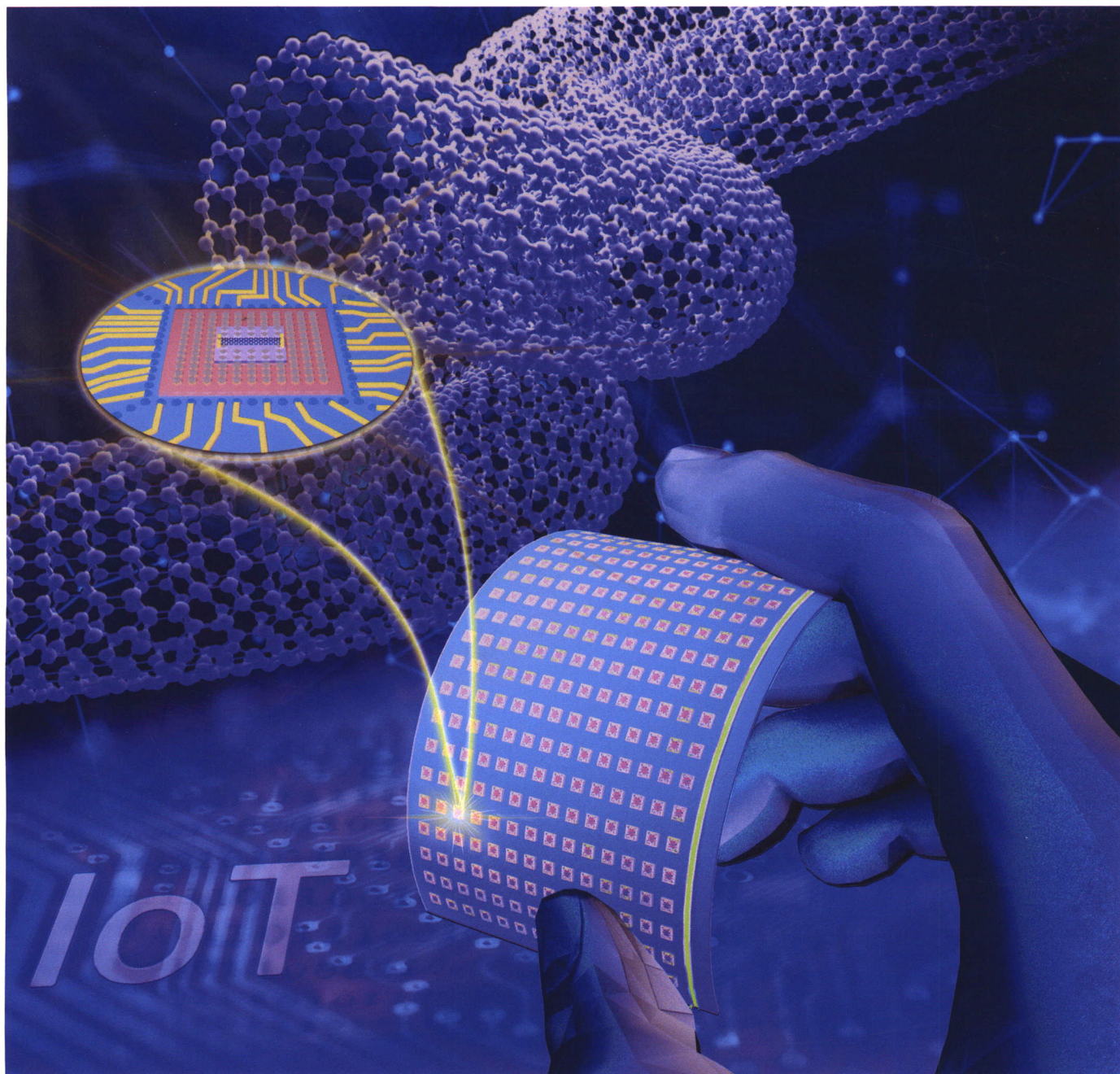
ISSN 1998-0124

CN 11-5974/O4

Nano Research

Volume 15 · Number 5 · May 2022

(Monthly, started in 2008)



纳米研究 (英文版) (月刊, 2008年创刊) 第15卷 第5期 2022年5月出版

Editors-in-Chief Yadong Li, Shoushan Fan

Sponsored by Tsinghua University & Chinese Chemical Society

Edited by Nano Research Editorial Office

Published by Tsinghua University Press

Address Xueyan Building,
Tsinghua University,
Beijing 100084, China

Website www.theNanoResearch.com & www.springer.com/journal/12274

Online Manuscript Submission, Review and Tracking System www.editorialmanager.com/nare

主管单位 中华人民共和国教育部

主办单位 清华大学

中国化学会

主 编 李亚栋 范守善

编 辑 《纳米研究》编辑部

出版发行 清华大学出版社有限公司

印刷单位 北京地大彩印有限公司